Institute of Clinical Sciences, Department of Biomaterials,

Göteborg University, Göteborg, Sweden

ON BONE REGENERATION IN POROUS BIOCERAMICS

Studies in humans and rabbits using free form fabricated scaffolds

Johan Malmström

Göteborg 2007

To Charlotte

ABSTRACT

The objective of the present thesis was to evaluate the effect of material chemistry and macro- and micro-porosity on bone regeneration in association with synthetic, porous ceramic materials. Ceramic scaffolds were designed and manufactured for experimental and human studies using free form fabrication (FFF), a technique which produces the object layer by layer using data from CAD files. The identical macroporous scaffolds of different chemistry and microporosity were created through control of the FFF and colloidal shaping processes.
The chemical composition of scaffolds was characterized by X-ray diffraction. Porosity was measured by Archimedes´ principle and the macroporosity of the scaffolds calculated from geometrical dimensions of the scaffold. Roughness of the macropores was investigated by scanning electron microscopy (SEM) and optical interferometry. The bone response to scaffolds made of zirconia and hydroxyapatite (with and without an open microporosity), inserted in rabbits and humans, were investigated at the light microscopical (LM) level. SEM, focussed ion beam microscopy (FIB) and transmission electron microscopy (TEM) were used for material-tissue interfacial analyses. A significantly greater bone ingrowth and direct bone contact were demonstrated inside macroporous scaffolds of hydroxyapatite compared to zirconia after 6 weeks in rabbit tibia and femur. The addition of open microporosity to hydroxyapatite provided an added, bone-promotive effect. Due to the FFF manufacturing process two different surface roughness values were obtained inside each macropore but no significant differences in bone contact were detected. The FIB technique to prepare intact samples for transmission electron microscopy was successfully applied on interfaces between bone and ceramic scaffolds. In zirconia a direct contact between the material and bone could be seen after 6 weeks in rabbit femur. For hydroxyapatite scaffolds, an apatite layer was demonstrated between the material and bone which was not present in the case of zirconia. The addition of micropores to the hydroxyapatite material reduced the width of the apatite layer from 200 nm to 100 nm. Furthermore, ingrowth of mineralized collagen fibrils could be detected inside the micropores. In the human study, the results from the two animal studies could be verified with respect to promotion of the bone response due to material and geometry, i.e. hydroxyapatite scaffolds were associated with a significantly greater bone regeneration than zirconia after 3 months in the human maxilla. Similar to observations in rabbit bone, a close contact was demonstrated between bone and hydroxyapatite and zirconia, respectively. In addition, ingrowth of bone was detected in the micropores of hydroxyapatite.
The FFF technique has enabled the production of ceramic scaffolds with controlled material properties, allowing systematic studies on the effects of material properties on bone regeneration in vivo. The results of the present studies show that bone ingrowth and bone contact is promoted in macroporous FFF ceramic scaffolds, in particular hydroxyapatite with an added open microporosity, hence providing FFF as a new, valuable research tool and a means to contribute to the clinical treatment of compromised bone conditions.

Keywords. bone regeneration, hydroxyapatite, zirconia, macroporosity, microporosity, free form fabrication, focused ion beam, scanning electron microscopy, transmission electron microscopy, rabbit, human

ISBN 978-91-628-7207-6

Correspondence. Johan Malmström, Department of Biomaterials, Institute of Clinical Sciences, Sahlgrenska Academy at Göteborg University, Box 412, SE 405 30 Göteborg, Sweden, E-mail: johan.malmstrom@biomaterials.gu.se

LIST OF PAPERS

This thesis is based on the following papers, which will be referred to in the text by their Roman numerals (I-IV):

I Johan Malmström, Erik Adolfsson, Lena Emanuelsson and Peter Thomsen
Bone ingrowth in zirconia and hydroxyapatite scaffolds with identical macroporosity
J Mater Sci Mater Med, in press

II Johan Malmström, Erik Adolfsson, Anna Arvidsson and Peter Thomsen
Bone response inside free form fabricated macro porous hydroxyapatite scaffolds with and without an open microporosity
Clin Impl Dent Relat Res, in press

III Johan Malmström, Tobias Jarmar, Erik Adolfsson, Håkan Engqvist and Peter Thomsen
Structure of the interface between bone and scaffolds of zirconia and hydroxyapatite
In manuscript

IV Johan Malmström, Christer Slotte, Erik Adolfsson, Ola Norderyd and Peter Thomsen
Bone response to free form fabricated hydroxyapatite and zirconia scaffolds. A histological study in the human maxilla
In manuscript

CONTENTS

INTRODUCTION 8

Bone 8

Biological bone grafts 9

Synthetic bone graft substitutes 9

Ceramics 10
Calcium phosphates 10
Hydroxyapatite 11
Oxides 12

Porosities of ceramics 12
Macroporosity 12
Microporosity 13
Mechanics of porous ceramics 14

Interface morphology/reactions to bone and material 14
Focused ion beam (FIB) 14
Interface analyses in general 15
Interface of inert materials and bone 15
Interface of bioactive materials and bone 17
Interface of pores 17

Shaping 18

Sintering 18

Free Form Fabrication 19

AIMS 22

MATERIALS AND METHODS 23

Free Form Fabrication of ceramic scaffolds 23

Material characterisation 24
Composition 24
Porosity 24
Roughness 25

Sterilization and endotoxin content of materials 25

Animals 25
Surgical procedure and anaesthesia, animal studies (I-III) 25

Humans 27
Inclusion/ exclusion criteria 27
Surgical procedure and anaesthesia, human histological study (IV) 27

Tissue preparation and sectioning techniques 28
Sample preparation for light microscopy (I-II, IV) 28
Sample preparation for scanning electron microscopy (I-IV) 29
Sample preparation for focused ion beam microscopy/ transmission electron microscopy (III) 29

LM morphometry 31
Animal studies (I-II), human study (IV) 31

Statistics (I-II,IV) 31

RESULTS 32

Materials 32
Chemical composition 32
Surface topography 33
Sterility and endotoxin content of materials 35

Macroscopical observations 35

Histology 35
Light microscopy 35
Scanning electron microscopy 37
Transmission electron microscopy 38

Histomorphometry (LM) 39

DISCUSSION 41

Role of material chemistry on the bone response in porous ceramics 41

Role of macro and microporosity on bone response in ceramics 42

Aspects on models and methods 44
Animals 44
Humans 44
Design of scaffolds 45
Histology 45
SEM/FIB/TEM 45

Aspects on Free Form Fabrication 46

Future 46

SUMMARY AND CONCLUSIONS 47

ACKNOWLEDGEMENTS 48

REFERENCES 50

PAPERS I-IV

INTRODUCTION

The necessity to replace bone in defects of the skeleton has long been a central part of clinical practice. Over the last decades, a great deal of research has focused on therapies for enhancing bone regeneration, closely linked to the evolution of bone surgery. Much progress has also been made simultaneously with an improved understanding of bone healing, leading to the elaboration of techniques targeting various factors involved in bone regeneration.

Bone

The skeleton is composed of two types of bone tissue, cortical and trabecular.
Cortical bone, also called compact bone, forms a protective outer shell around every bone and constitutes approximately 80% of the skeletal mass. Trabecular or cancellous bone is located beneath the cortical bone. The intricate mesh of trabecular bone forms the interior scaffold that helps bone to maintain its shape when exposed to compressive forces.
The two types of bone cells participating in the remodelling of bone, osteoclasts and osteoblasts, have diametrically opposed actions which are influenced by numerous factors [1].
Osteoclasts, bone resorbing cells, rest directly on the surface subjected to resorption during activity. Osteoclasts are derived from the hematopoetic monocytic cell lineage [1].
Active osteoblasts secrete collagen fibrils and other extracellular matrix components together forming an unmineralized matrix (osteoid). Osteoblasts become completely embedded in the bone they produce and are then called osteocytes, which are no longer able to actively form bone.
Cortical and trabecular bone is created and re-created by the remodelling action of osteoblasts and osteoclasts which allows repair of damaged tissue and allows the adaptation of bone structure to altered loading condition. Remodelling begins with resorption by osteoclasts which secure themselves to bone surfaces and tunnel into the bone. The next step is bone formation; osteoblasts are attracted to the cavities formed by the osteoclasts and filling the cavity with osteoid. The osteoid is then mineralized [1].
The ability of bone to regenerate rather than form scar tissue is a well-known characteristic of bone, which produces a structure physiologically and biomechanically indistinguishable from the original. The dynamic interactions among cells and cell-derived molecules at a fracture site ensure complete regeneration of bone. The bone repair process begins with an inflammatory response (with neutrophils and macrophages) present that causes granulation tissue to proliferate into the wound site. It is through the granulation tissue that capillaries, fibroblasts and osteoprogenitor cells are brought into the wound site. Over time the newly formed woven bone is remodelled and replaced by lamellar bone.

Biological bone grafts

Bone transplants are today routinely used in humans to promote fracture healing, enhance joint fusion, and repair bone defects. Fresh autogenous grafts are still considered a "golden standard" because of their lack of immunogenicity.

It was not until the nineteenth century that the clinical usefulness of bone grafting was recognized. The first recorded human autogenous bone grafting was described in 1820 and in 1867 the scientific principle of bone grafting was formulated [2,3]. In the early 1900s, the extensive research performed by Axhausen [4] on the transplantation of periosteum, marrow, and bone in rats, rabbits, and dogs provided a foundation of knowledge that even today remains largely unchallenged. Barth was the first to describe the process of new tissue invading along channels created by invasive blood vessels or along pre-existing channels in the transplanted bone [5]. This process was called "schleichender ersatz", a term literally translated by Phemister in 1914 as "creeping substitution", to describe a dynamic reconstruction and healing process for bone transplantation [6].

Biological bone grafts can be separated in three groups. 1) Autografts: bone grafts harvested and transferred within an individual, 2) Allografts: bone grafts harvested in one individual and transferred to another individual of the same species [7-10] and 3) Xenografts: bone grafts harvested and transferred between different species. The most common xenografts are harvested from bovine bone and processed to obtain the bone mineral without the organic component [11], however the risk of transmission of diseases has been a topic for discussion [12].

Three basic principles exist in which bone grafts are suggested to stimulate new bone formation [13]; (1) osteogenesis**,** the formation of bone from surviving bone cells within the graft [13], (2) osteoinduction, a process where mesenchymal cells of the host are recruited by various molecules [13] to differentiate into osteoblasts and (3) osteoconduction which refers to the process of tissue growth continuously along a surface of the graft [14,15].

The main disadvantages of bone grafts are the only limited amounts of autogenous bone that can be harvested, the additional surgical intervention needed and the primary resorption after placement of the graft [16,17]. Also complications from the donor site has been reported [18,19].

Synthetic bone graft substitutes

Clinical use of osteoconductive materials, has gained much interest. The major contribution to the field of osteoconduction made in the 20th century consisted of the development of synthetic agents. Coupled to an increase in clinical bone graft procedures is an increasing usage of different types of materials. New materials and applications are continuously being tested in the laboratory as well as clinically. As a result, different materials and forming methods have been proven best suited for certain demands and applications.

A suitable synthetic bone substitute may reduce, or in some cases, eliminate the need of bone grafting, thereby avoiding the disadvantages associated with bone grafts.

Among the advantages of synthetic bone substitutes are unlimited amount, it precludes an additional surgical site, involves no risk for disease transmission and allows design and prototype testing of different materials and geometries to further promote the bone response.
Generally, osteoconductive materials provide a passive scaffold onto which osteoprogenitor cells can lay new bone. Osteoconductive agents today include ceramics, collagen, porous metals, polyglycolic and polylactic acid polymers, and bioactive glasses [20]. Many of these materials are used as fillers in bone surgery. They can also function as carriers for growth factors and antibiotics, and may be presented as blocks, fibers, granules, powders, gels, and sprays, depending on the application. The properties of osteoconductive synthetic grafts will therefore be determined by their physical presentation as well as other factors, such as chemical composition, processing and interconnective porosity.
Clinically, the understanding of which factor(s) are deficient in a given patient determines the criteria for selecting a specific regenerative therapy. If synthetic bone grafting is the answer, good knowledge about parameters affecting the bone response will guide the ultimate choice. In difficult cases, several contributing factors can be identified and a combination of therapies required. It is unlikely that one grafting agent will eventually be found to optimally resolve all reconstructive conditions where bone formation is challenged. Individual types of grafting materials are likely to improve in their biomechanical and biological performance and it is possible that combinations of different materials will provide new solutions to specific clinical issues. A thorough and long-term evaluation of new biomaterials is needed to verify their advantages over clinical controls and prevent side-effects such as transmission of pathogens or unpredictable resorption of the implant and newly formed bone.
Even though there is a large variety of an osteoconductive material available most synthetic bone graft substitutes are calcium based ceramics. However, it is beyond the scope of this introduction to give a complete listing of all bone substitutes, but rather to present the materials used in the present thesis.

Ceramics
Ceramics are virtually all materials that are inorganic and not metallic. With other word this means that brick, glass, porcelain, carbon, cement, rocks and minerals are ceramic materials. Ceramics have become a diverse class of biomaterials during the 20th century. Ceramics used in medical applications can be divided in two large groups: The technical high strength ceramics used in load bearing situations like zirconia in dental caps and ball heads of total hip replacements and the calcium phosphate based ceramics like hydroxyapatite used for bone regenerative applications [21].

Calcium phosphates
Calcium sulphate (plaster of Paris) was one of the first materials investigated as a synthetic osteoconductive bone graft substitute [22]. However, concerns were raised over the, poor osteoconductive properties, of plaster of Paris, and its clinical use declined [23]. The interest

in calcium phosphate as hard tissue implants initially evolved around the suggested release of calcium ions that would stimulate osteogenesis [24] and the chemical similarity towards bone. Several phases of calcium phosphate ceramics are available with different Ca/P ratios [25] (Table I). The stability of calcium phosphate ceramics depend considerably upon phase, porosity, microstructure and environment [26]. These calcium phosphate materials can also be prepared with a continuous range of calcium/phosphate ratio without the presence of crystal structure. However, these amorphous calcium phosphates are not equivalent to the crystalline calcium phosphates except for the similar chemical composition. The two most common calcium phosphates evaluated as bone substitutes are hydroxyapatite and tricalcium phosphate. Among the calcium phosphates apatites have the lowest solubility and thereby resorb slowly (within years), if at all. Tricalcium phosphates have a higher solubility and have been found to resorb within days to week in vitro and in vivo [27].

Table I
Ca/P ratio, chemical formula and name of different calcium phosphates

CaP	Formula	Chemical (mineral) name
0.5	$Ca(H_2PO_4)_2\ H_2O$	Monocalcium phosphate monohydrate
1.0	$Ca(HPO_4)\ H_2O$	Calcium phosphate dihydrate (Brushite)
1.0	$CaHPO_4$	Calcium phosphate (anhydrous) (Moneite)
1.33	$Ca_4H_2(PO_4)_3\ 2.5H_20$	Octacalcium phosphate (OCP)
1.5	$Ca_3(PO_4)_2$	Tricalcium phosphate (TCP)
1.67	$Ca_{10}(PO_4)_6(OH)_2$	Hydroxyapatite (HA)
2.0	$CaO\ Ca_3(PO_4)_2$	Tetracalcium phosphate monoxyde

Hydroxyapatite

Hydroxyapatite is the main component of the mineral matrix of bone [28]. The bone-like composition, structure [29-31], combined with an excellent biocompatibility [31] and the possibility to obtain physiochemical bond with newly formed bone [28] has led to an increased clinical use of hydroxyapatite over the last 30 years [31]. Apatites of natural and synthetic origin are today used as bone substitutes. Materials of natural origin is derived from bovine bone [32]. These materials are not pure but contain some of the minor trace elements originally present in the bone [33]. Synthetic materials $Ca_{10}(PO_4)_6(OH)_2$ are prepared by precipitation under basic conditions and subsequent sintering usually at temperatures above 1000ºC [33]. Hydroxyapatite materials can be used as sintered structures, as granules, as composites [33,34] or as a coatings [26].

Oxides

The structural ceramics most commonly used are alumina and zirconia. Generally, both alumina and zirconia oxides have characteristics of high hardness, high abrasion resistance, strength and chemical inertness. These properties have made them considered as bioinert ceramics for high strength dental applications and bone implants. The biocompatibility of alumina and zirconia have been evaluated and the materials have been considered to become osseointegrated when used as dental implants [35-38]. The mechanical characteristics of alumina implants produced in the mid-seventies were considered non-sufficient for long-term loading and dental implant products had initial mechanical problems. Therefore, the research on the use of zirconia ceramics as biomaterials commenced about twenty years ago and zirconia has now been in clinical use as ball heads of total hip replacement [39] and developments are in progress for applications in other medical devices [37]. Zirconia occurs in three forms: monoclinic, cubic and tetragonal. Pure zirconia is monoclinic at room temperature. By the addition of "stabilising" oxides, like CaO, MgO, CeO_2, Y_2O_3, also the tetragonal and cubic phase can be maintained at room temperature. Zirconium dioxide can thereby occur in stabilized and partially stabilized form. The high strength not seen in other ceramics can be explained by the transformation toughening mechanisms operating in the microstructure of tetragonal zirconia. In regions of crack propagation, a local transformation occurs from the tetragonal to the monoclinic phase because of the internal stresses. At the crack a local volume expansion results counteracting crack propagation. More energy, i.e., higher forces, is then necessary for the crack to continue. Though, the crack does not go away, it does not propagate any further at that specific time. This results in improved fracture toughness and strength.

The oxide layer that naturally forms and protects an underlying, highly reactive metal, e.g. titanium, against uncontrolled further oxidation may also be regarded as a ceramic.

The biocompatitbility of titanium is therefore partly a direct consequence of the properties of its thin oxide film that protects the metal from further chemical or biological reactions and corrosion.

Porosities of ceramics

Macroporosity

Porosity is defined as the percentage of void space in a solid [40] and it is a morphological property independent of the material. Pores are necessary for bone tissue formation because they allow migration and proliferation of osteoblasts and mesenchymal cells, as well as vascularization [41]. In addition, a porous surface improves mechanical interlocking between the implant biomaterial and the surrounding natural bone, providing greater mechanical stability at this critical interface [42]. Even though there has been an interest to determine the optimum pore structure [43-48] in materials used as bone substitutes, there is still limited knowledge about the mechanisms behind bone ingrowth, or osseointegration, within macroporous materials [43-46,49-58]. Introducing controlled porosity in calcium phosphates [59] is not easy and

several manufacturing techniques have been developed for making porous hydroxyapatite. The information available in the literature is not sufficient to suggest a general guide for optimal bone-tissue outcomes. This is mainly due to the wide range of bone features in vivo and the diversity of substitutes with less well defined porosity. In addition, the results might also depend on the rate of resorption of the investigated bone substitute [60], which makes it almost impossible to compare the bone response between different porous ceramic materials. However, some remarks can be provided based on the literature. The requirement of highly porous implants for bone regeneration is solidified by the absence of any reports on the beneficial effects of lower porosity scaffolds in vivo. High porosity [42,61,62] and large pores [63-65] thereby enhance bone ingrowth and osseointegration of the implant after surgery. The minimum recommended pore size for a scaffold is 100μm based on the early work of Hulbert et al.[66], but subsequent studies have shown better osteogenesis for implants with pores > 300μm [63-65]. Furthermore, other researchers have suggested the importance of additional structural parameters, such as pore morphology and pore connectivity [43,45,46,57,58] to promote the bone response. There are also a limited numbers of reports in the literature that show no effect of porosity on the amount of appositional bone [67,68].

Microporosity

Materials with pore sizes in the micrometer range are often termed microporous materials. The microporosities are located between ceramic grains after sintering, as the heating – and manufacturing process does not completely densify the material. When the sintering temperature is changed in order to vary the microporosity in ceramic materials other material characteristics such as grain size will be changed. For calcium phosphate materials the temperature change can also influence both phase and chemical composition of the prepared material. This indicates that it is not obvious how to vary the microporosity during fabrication without influencing other characteristics of the scaffold. In vivo results indicate that manipulation of the levels of microporosity within hydroxyapatite scaffolds can be used to accelerate osseointegration [69]. On the other hand, results have also demonstrated no differences in bone response to hydroxyapatite with different levels of microporosity [70].

The uncertainty regarding the effect of microporosity on the bone response might indicate the need of improved characterisation of micropores, test models and evaluation techniques. The suggested mechanisms in the literature whereby the level of microporosity accelerates the bone response are many. Firstly, a general idea is that the established connections due to micropores improves transportation and circulation, thereby facilitating blood vessel and tissue ingrowth into the hydroxyapatite [45]. Secondly, through an initial combination of enhanced angiogenesis [71] and cell adhesion [72,73], the sensitivity of bone cells has been suggested to be altered [71,72]. In the long term, the influence of both micro and macro porosity on bone adaptation appear to play a role [74,75]. Thirdly, by affecting the interface dynamics, micropores are suggested to make the material osteoinductive in the way that relevant cells are triggered to differentiate into osteogenic lineage [76]. Finally, the microporous surface is

also suggested to modulate the adsorption of proteins and further the adhesion and proliferation of human bone cells [77].

Mechanics of porous ceramics

The mechanical behaviour of ceramics will influence their application as an implant in the human body. Generally, the strength of a ceramic material is based on the material fracture toughness and the largest most loaded defect [21]. A ceramic material can have large span in strength between different test bodies, compared to metal where the span in strength seldom is larger than about one percent [21]. The explanation to the variation in strength is found when regarding the ceramic material as a chain. The weakest link makes the chain fail at sufficient load. To interpret material data for ceramics can be more difficult than for many other types of materials since the results are sample specific depending on the: sample size, forming method, test method and preparation of the test slip [21].

All ceramic materials are significantly stronger in compression than in tension. For ceramic scaffolds, the tensile and compressive strength and fatigue resistance also depend on the total volume of porosity. As mentioned earlier, porosity can be in the form of micropores or macropores. There is, however, an upper limit in porosity and pore size set by constraints associated with mechanical properties. An increase in the void volume results in a reduction in mechanical strength of the scaffold, which can be critical for regeneration in load-bearing bones. The extent to which pore size can be increased while maintaining mechanical requirements is dependent on many factors including the nature of the biomaterial and the processing conditions used in its fabrication.

Compression testing has established that bone ingrowth has a strong reinforcing effect on porous implants, which is more pronounced in lower density implants as a result of a greater relative volume of bone ingrowth [58] [51] [78] [79]. Regarding the effect on load bearing properties of microporous hydroxyapatite scaffolds, compressive strength of scaffolds without microporosity is significantly greater than the scaffolds with microporosity [80]. However, bone has been shown to effectively arrest crack propagation in microporous hydroxyapatite scaffolds [81].

Interface morphology/reactions to bone and material

Focused ion beam (FIB)

It is essential in transmission electron microscopy (TEM) that the sample preparation procedure creates as little damage as possible [82,83]. The standard technique for preparing biological TEM samples containing hydroxyapatite is by ultramicrotome, i.e. sectioning ultra thin (10-90 nm) sections with a diamond knife and collecting them in a water trough. An advantage so far of ultramicrotome over ion milling (not using a focused beam) is the relative ease by which samples can be sectioned. Hence, it is the only feasible technique that is widely available for preparing multiple samples. However, the main setback using the ultramicrotome process are

the artefacts produced in the structure of sections due to the technique [82]. For this reason the Focused Ion Beam (FIB) system, where such impact related damage is minimal, was introduced in the field of materials preparation for transmission electron microscopy.
Focused ion beam (FIB) microscopy has been used extensively in the material science community and within microelectronics industry [84,85]. The FIB system scans a beam of positively charged gallium ions over the sample, similar to the electron beam in the scanning electron microscopy (SEM). The ions generate sputtered neutral atoms, secondary electrons, and secondary ions. The electrons or the positively charged ions can be used to form an image. More significantly it is possible to increase the beam current of the primary ion beam and use the FIB as a fine-scale micro-machining tool, for example, to easily find regions of interest and to cut TEM samples with very high accuracy receiving intact samples of the interface [86].

Interface analyses in general

Analysis of the behaviour of bioactive materials shows that optimal clinical success is due to the formation of a stable, mechanically strong interface with both bone and soft connective tissue [87]. The mechanism of tissue attachment is directly related to the type of tissue response at the implant interface [87].
In vivo, bioactivity is defined as the property of the material to develop a direct, adherent, and strong bonding with the bone tissue [88-90]. This property was originally observed with silica-based glasses with special formulation referred to as bioactive glass and associated with a CaP-rich layer ("apatite layer") that forms between the bioactive glass and the bone tissue [88,89]. The concept of chemical bonding is based on the findings that the apatite crystals in the bone and the crystals in these apatite layers are intermingled at their interfaces, suggesting chemical bonding in a broad sense between these surface-active ceramics and bone [91]. In vitro on the other hand, bioactivity has been attributed to materials that have the ability to form carbonate hydroxyapatite on its surface when exposed to simulated body fluid (SBF) [92-94]. The use of SBF is not an exact replica of the in vivo environment. Further, differences between the in vitro environment using SBF and in vivo have been demonstrated for e.g. zirconia [95,96]. Also there are materials that do not form an apatite layer either in vivo or in vitro. This is the case for â - tricalcium phosphates [97,98].

Interface of inert materials and bone

Interface studies will provide data concerning biocompatibility, biofunctionality, bioactivity and biodegradation leading to a greater insight into the mechanisms of bone bonding at the ultrastrucural level improving the design of scaffolds with different morphology and chemistry.
No material implanted in living tissue is inert; all materials elicit a response from living tissue. There has been a general idea that when biomaterials are almost inert and the interface is not chemically or biologically bonded, there is relative movement, and progressive development of a nonadherent fibrous capsule in both soft and hard tissues. Movement of the interface

eventually leads to deterioration of the tissue at the interface and function of the implant [87]. Bioactive ceramics have been reported to have better osteoconductive potential than bioinert ceramics [99,100] and the differences between bioactive and bioinert ceramics has been suggested not to lie in the amount of bone formed but in the lack of a fibrous tissue seam in the interface between the bioactive implant and the new bone [101]. Furthermore, by evaluating in vitro data it has been suggested that zirconia ceramics, are not as effective as hydroxyapatite in accelerating growth and differentiation of osteoblast-like cells and that this is most probably due to the chemical and physical instability and composition of hydroxyapatite [102].
Regarding the ultrastructure and possible mechanisms at the zirconia/bone interface in vivo the literature is sparse. There is however both human [37] and animal [103-106] LM data available demonstrating osseointegration of threaded zirconia implants. In animals the LM histology showed high degrees of bone-implant contact. Sennerby et al [38] has also compared zirconia implants with different surface modifications to evaluate the bone contact and bone ingrowth in an rabbit model. No differences in bone –implant contact or bone areas filling the threads were observed. Zirconia dental implant in humans has been evaluated by Mellinghof [37]. In a clinical study 189 implants (type Z3, Z-System AG) were implanted and the results presented by the author suggested that when compared to similar studies with titanium implants, zirconia implants did comparably well. Though, of the 189 implants placed – nine were explanted and one implant fractured on loading.
The only high resolution study available on zirconia except the one presented in this thesis applied zirconium oxide films fabricated on silicon wafers using a filtered cathodic arch system in concert with oxygen plasma. The results showed bone-like apatite formed on the surface of the zirconia thin film in SBF immersion experiments. The author suggests that the naonstructured surface is believed to be the key factor that apatite is induced to precipitate on the surface [95]. Since zirconia and titanium oxide are chemically similar materials it is of interest to shortly review the ultrastructure of the titanium oxide/ bone interface. Transmission electron microscopy analysis of screw-shaped titanium implants from rabbits as well as of clinically retrieved specimens have revealed that mineralized bone never came in true direct contact with the implant surface. There was always a 100- to 500 – nm – thick interposed layer with a dens amorphous substance, irrespective of time after implantation [107,108]. According to a review by Albrektsson et al. [109], it seems that all authors who have tried to describe the bone-titanium interface (not using FIB) at the ultrastructural level have come to the same conclusion: there is one type of amorphous layer in the bone-to-metal interface, even if the width and the content (mineral, collagen, proteoglycans) has been debated.
The general lack in high resolution studies dealing with zirconia as an implant in contact with bone can be due to the earlier applications as a biomaterial were bone contact situations was not present or the goal of the treatment.

Interface of bioactive materials and bone

Different reaction patterns have been suggested to take place at the hydroxyapatite-bone interface [31,110-112]. Bone has been reported to bond directly to hydroxyapatite either by the establishment of an organic-free transition layer comprising biological apatite with a thickness up to 1000 nm [113] or as a result of the initial adsorption of proteins and glycosaminoglycans [114]. Investigators have also reported bone growth on sintered hydroxyapatite, both with and without an intervening apatite layer [115].

The outer layer that hydroxyapatite characteristically demonstrates has been reported to consist of carbonate-apatite crystals with a defective structure, by which the apatite structure is most important since it resemble bone apatite crystals [116-118]. Therefore, once this layer is formed on the material surface, new bone formation along the surface may be easier. It has been suggested that this layer has a more active role [94], preferentially adsorbing proteins and that the proteins serve as growth factors. A common characteristic of bioactive glasses and bioactive ceramics is a time-dependent modification of the surface that occurs upon implantation [94,119,120]. The surface forms a biologically active hydroxycarbonate apatite layer that provides the bonding interface with the tissue [87]. It is generally very difficult to distinguish the crystals of the surface apatite layer with those of the immature bone in hydroxyapatite specimens. In both the apatite layer and the immature bone, the crystals are basically the same carbonate-containing hydroxyapatite with a defective structure, and the surrounding environment in which apatite precipitation occurs is the same. Therefore the difficulty in distinction may be a natural consequence, although the surface structure of hydroxyapatite crystals and adsorbed proteins on hydroxyapatite may affect the formation of the surface apatite layer [98]. Ogiso and co-workers [121,122] have shown, through TEM lattice image analysis of dense hydroxyapatite bone interfaces, an almost perfect epitaxial alignment of the growing bone crystallites with the apatite crystals in the implant. Osborn [123] stated that this direct and firm bond finds its origin in bilateral crystal growth originating from both the bone apatite and the crystal phase of the ceramic.

Interface of pores

Relatively few studies have compared the structure of bone at the bone-material interface to that within the material [74]. Earlier studies have shown that no evident difference was found between interface characteristics of dense and macroporous hydroxyapatite to bone [28]. It was explained by the authors that this was due to that both materials possess the same surface properties [28]. Recent results with respect to the effect of micropores has suggested that organized, mineralized collagen fibrils had grown into the strut porosity (Ø 3μm) at the interface between the macroporous hydroxyapatite implant (Ø 100-200μm) and the surrounding bone. In comparison, deeper within the implant, disorganized and unmineralized fibers were observed within the strut porosity (Ø 3μm) [83]. It was also suggested that the ingrowth of collagen fibrils into outer micropores stabilizes the interface between the porous scaffold and the surrounding bone tissue.

Shaping

The lack of controllability in the ceramic materials offered on the market makes assumptions whether a certain property of the material has an effect on the bone response almost impossible. Today, new ways of designing the ceramic material allow a control and optimization of design parameters. The ways of controlling the ceramic material can be divided in two major groups: shaping and sintering. Ceramics, with the exception of glass, are often produced by powder technology. This means that one pre-shape (form) a so called green body through different techniques. The green body is thereafter sintered, which is made through a heating process. Common industrial forming methods for ceramics are powder compaction and colloidal shaping techniques (Table II).

Table II

The process of powder compaction and colloidal shaping

Powder compaction	Colloidal shaping (slips)
Powder	Powder+water+additions
Compaction (green body)	Slip preparation
Processing	Moulding of component (green body)
Sintering	Sintering

Since ceramics shrink during sintering care must be taken during the formation of the green body. Often the shrinkage is not uniform and a final finish must be added if the levels of acceptance is high. The final finishing of ceramics is not always easy for several reasons, cracks can easily be induced, and several materials are extremely hard. The different forming methods have all different drawbacks with respect to possible geometry. The forming methods will also influence the strength and Weibull modulus of the material [21].

Sintering

The sintering process makes the powder granules bind to each other. Since the green body always contain an amount of porosity there is always shrinkage during the sintering process. When there is a desire of achieving strong materials, a total absence of pores must be achieved. Some ceramics are hard to sinter. For these materials, alternative sintering processes have been developed [21].

Free Form Fabrication

For many years, developments in the field of biomaterials generally involved trial-and-error experiments [124]**.** This approach has often been successful, and over the last 30 years, more than 40 different ceramic, metal, and polymeric materials have been used to replace, repair, or augment more than 40 different parts of the human body [125,126]**.**

In order to explore the role of the internal architecture on the biological behaviour of porous ceramic implants, traditional processing methods provide a minimal control in this regard [48]. Traditionally, the internal pores in these ceramics (hydroxyapatites) are either obtained from the coralline exoskeletal [53] patterns and bovine bone [32] or from the embedded organic particles in the starting hydroxyapatite powder [127]. Today there are alternative ways of producing sophisticated ceramic objects directly from computer aided design (CAD) files using a class of technologies commonly referred to as Free Form Fabrication (FFF**)** [128] or rapid prototyping (RP) [129]**.** Free Form Fabrication is an "additive" process compared to most machining processes (milling, drilling, grinding, etc.) which are "subtractive" processes that remove material from a solid block (Fig 1). The additive nature of Free Form Fabrication allows the object to grow layer by layer and to create objects with complicated internal features which are impossible to achieve with conventional methods [130]. The starting point for Free Form Fabrication is the solid or surface model. It defines what is to be built. A model for mechanical parts is created by a designer with a standard CAD package. Models for anatomical objects can be generated from medical computed tomography (CT) or magnetic resonance imaging (MRI) files using appropriate software. The solid model is then put into a more easily handled form, an "interprocess model". Most commonly, the surface of the CAD model is approximated by a tessellation of triangles, in a "stereolithographic (STL) format" which is the de facto standard form of many Free Form Fabrication systems. Some information is lost in this approximation, but the relative simplicity of the STL triangle format makes it easier to do the subsequent calculations. The Free Form Fabrication software uses the STL surface to create a set of "slice files", whereby the solid object is converted into many slices, each representing a layer to be built. The slice files are then used to generate a set of "build files" which have the instructions for building each layer. These building files are different for each Free Form Fabrication method. Although several Free Form Fabrication techniques exist, all employ the same basic five-step process. The steps are:

1. Create a CAD model of the design
2. Convert the CAD model to STL format
3. Slice the STL file into thin cross-sectional layers
4. Construct the model or mould one layer on top of another
5. Clean and finish the prototype/model

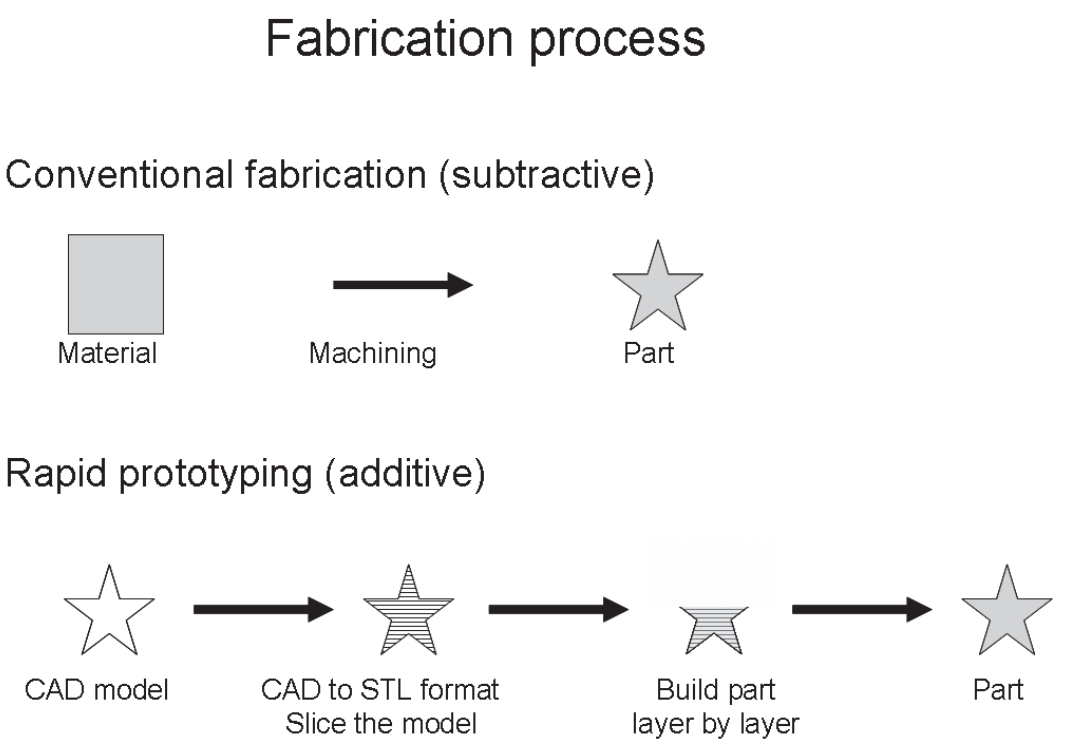

Figure 1
Subtractive vs additive fabrication process [131]

By creation of tangible prototypes of designs rather than just two-dimensional pictures such models have numerous uses. These prototypes make excellent visual aids and can be used as controlled research tools. In addition to prototypes, Free Form Fabrication techniques can also be used to make tooling (referred to as rapid tooling) and even production-quality parts (rapid manufacturing). The ability to create scaffolds directly from images raises the question as to the relevance of an optimization manufacturing protocol. Why not create scaffolds that just mimic existing trabecular bone structure? There would be a number of difficulties to this approach. First, if one desires the scaffold to match effective bone properties, the base biomaterial stiffness of the trabecular scaffold would have to match trabecular tissue stiffness itself. Second, scaffold porosity would be the same as the original trabecular structure, not allowing for alterations in scaffold porosity that may enhance osteogenesis. Third, the regenerate tissue within a trabecular architecture would be the negative of the scaffold structure of the native trabecular architecture; therefore matching neither the desired native structure nor mechanical properties The ability to design and fabricate scaffolds using the Free Form Fabrication technology, provides multiple possibilities to evaluate the role of scaffold design for tissue regeneration [132].

Free Form Fabrication is today widely used in the automotive, aerospace, medical, and consumer products industries. The current challenge is to create ceramic prototypes by allowing Free Form Fabrication methods to also make ceramics thereby also fabricating otherwise unobtainable objects. Other examples could be sensors with embedded electrodes and biomedical objects, built to fit a particular anatomical defect, grown to shapes by medical images (CT, MRI), perhaps with a sophisticated interior configuration [133]. Although the possible applications are virtually limitless, nearly all fall into one of the following categories: prototyping, rapid tooling, or rapid manufacturing. Because Free Form Fabrication technologies are being increasingly used in non-prototyping applications, the techniques are often collectively referred to as rapid prototyping; computer automated manufacturing, or layered manufacturing. The latter term is particularly descriptive of the basic process used by all Free Form Fabrication techniques.

AIMS

As a whole, very little is known about the effect of controlled material chemistry and porosity on bone regeneration. A major question is if these material parameters also will affect the ultrastructure of the interface between the implant and bone.
In order to be able to perform studies on these critical issues, it is judge necessary, firstly, to design and produce ceramic materials with techniques allowing controlled shape, form and porosity, and, secondly, to prepare intact interfaces of bone and porous ceramic materials. In the present thesis, using a standardized experimental model in rabbits and in the human maxilla, different aspects of the role of material chemistry and porosity for bone in- and on-growth were studied. The aims of the present thesis were:

- To evaluate how the material chemistry influenced the bone response in scaffolds with identical macroporosity.
- To evaluate how an open microporosity influenced the bone response in scaffolds with identical macroporosity and chemistry.
- To evaluate how the chemistry and microporosity of the material influenced the bone/biomaterial interface on an ultrastructural level.
- To verify animal data by evaluating the effect of material chemistry and open micoporosity on the bone response in scaffolds in the human maxilla.

MATERIALS AND METHODS

Free Form Fabrication of ceramic scaffolds (I-IV)

A CAD tool was used to design models of scaffolds with squarely shaped and interconnected pore channels (Fig 2A). In order to obtain scaffolds with the same size and macroporosity from the different materials, the size of the models were rescaled individually to compensate for the sintering shrinkage of each material. A Free Form Fabrication equipment (Model Maker II, Sanders, USA) using an inkjet printing principle was used to build moulds (Fig 2B) corresponding to the designed macroporosities with a layer thickness of approximately 50 µm. The Free Form Fabricated moulds were infiltrated with ceramic suspensions (Fig 2C) prepared by ball milling of hydroxyapatite (Plasma Biotal, UK) and zirconia (Tosoh, Japan) with a solids loading of 48 vol% and 50 vol%, respectively. The use of colloidal shaping processes made it further possible to vary the sintered density from almost fully dense materials to materials containing large volumes of microporosity by control of the shaping process. The cast materials were heated with a low heating rate of 1°C/min up to 600°C to burn away the mould and organic additives, and 5°C/min up to 1200°C for hydroxyapatite and 1500°C for zirconia. The sintering temperature was kept for 2 hours before the temperature was decreased by 5°C/min.

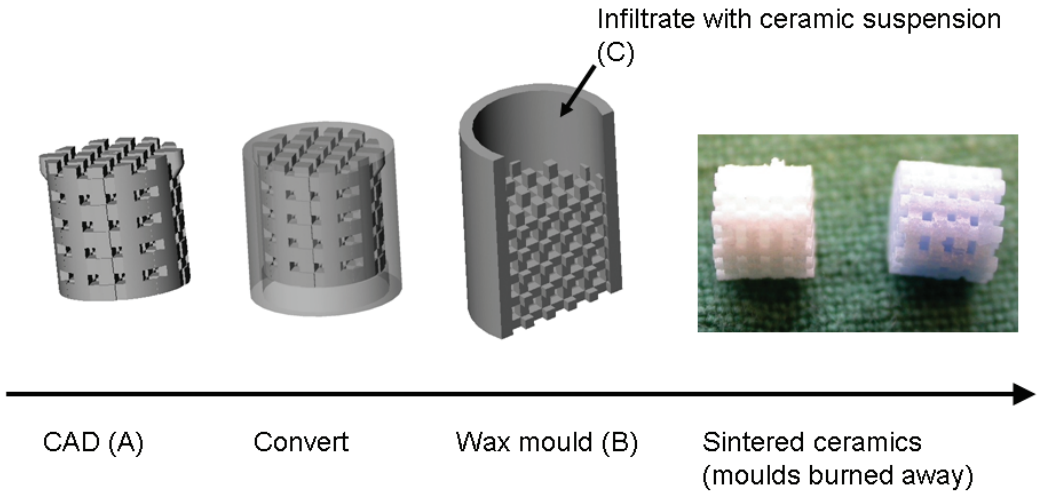

Figure 2 A-C

The CAD design (A) is used to produce Free Form Fabricated wax moulds (B) which are infiltrated with ceramic suspension (C) and finally sintered in order to receive sintered ceramics.

Ceramics representing each material were also produced in bar form to enable the surface analyses of the two sides created due to the manufacturing direction (Fig 3 A-C). This was done in study I-II where 3 ceramic bars (5 x 5 mm) of each material were synthesized according to the same protocol as described for the scaffolds.

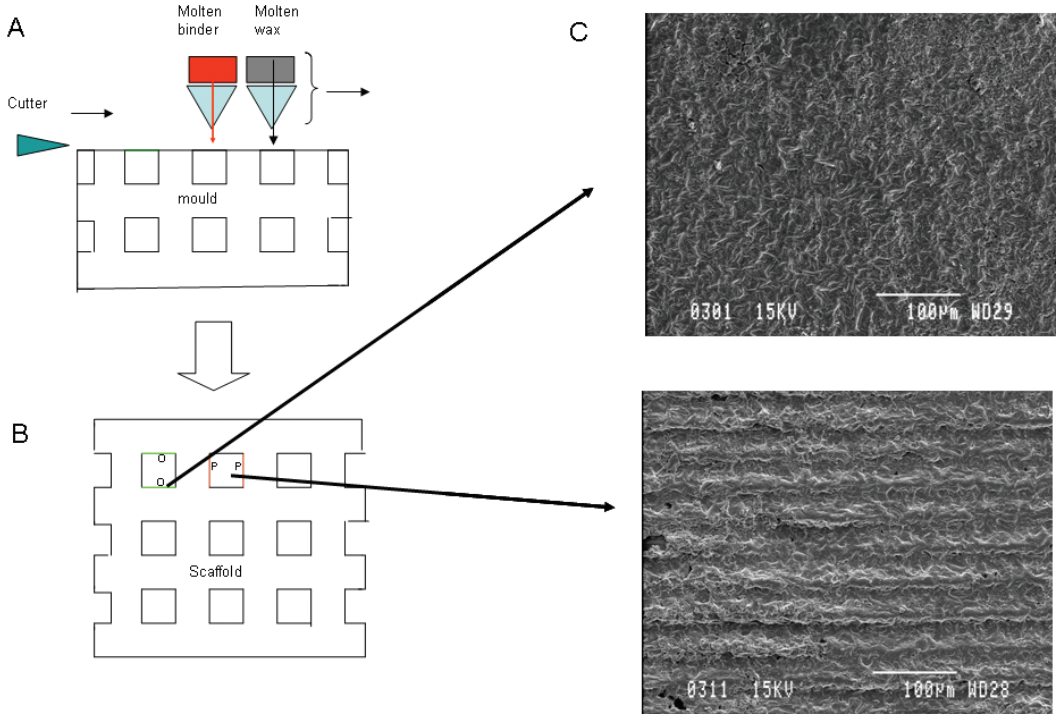

Figure 3 A-C
Schematic pictures (not to scale) illustrating the procedure which forms the surfaces of the macropore.
After each layer built by the two ink-jets a knife cuts the surface before repeating the process (A), thereby creating the two surfaces in each macropore built, one orthogonal (O) and one parallel (P) with the manufacturing direction (B,C).

Material characterisation

Composition

The sintered materials were characterized by their X-ray diffraction (XRD) patterns obtained in a Guinier-Hägg camera, using CuKα_1 radiation.

Porosity

The bulk porosity of the sintered materials was measured by Archimedes' principle and the macroporosity of the scaffold was calculated from the geometrical dimensions of the scaffolds.

Roughness

The surface of the sintered materials was studied by scanning electron microscopy (SEM) (JEOL JSM-840A, Tokyo, Japan) and optical interferometry (MicroXAM™, PhaseShift, Tucson, USA). The interferometry analysis was performed with a 50X objective and a zoom factor of 0.625, resulting in a measurement area of 200x260 μm^2. In total three specimens of each type of material were used for the topographical characterisation. Interferometer measurements were made on two beam surfaces of each material representing the inside of the macropores created by the manufacturing process, best referred to as: (P) – side, parallel to manufacturing direction and (O) – side, orthogonal to manufacturing direction (Fig 3 B,C). The topography of (P) and (O) sides were described as the mean of 30 measurements for each surface and material resulting in two surface roughness values for each scaffold material. The errors of form were removed with a digital Gaussian filter sized 50x50 μm^2 before calculating the following topographical parameters: (1) S_a - the average height of structures from a mean plane; (2) S_{ds} - the number of peaks per unit area; (3) S_{dr} - the developed surface ratio; (4) S_{tr} - texture aspect ratio used to separate isotropy and anisotropy of surfaces; (5) S_{ci} - the core fluid retention index.

Sterilization and endotoxin content of materials

The scaffolds were ultrasonically cleaned in acetone (10 min), and ethanol (99,5 %) for 3 x 10 min , and thereafter air dried. The scaffolds were placed in sterile packages and β– irradiation was used to sterilise the scaffolds at a dose of 2 x 20 kGy (Sterigenics, Espergaerde, Denmark)**.** The endotoxin content was determined for the scaffolds (I-IV) using Limulus Amebocyte Lysate (LAL) method.

Animals

All animal experiments were approved by the Local Animal Ethical Committee Göteborg University (Dnr. 237-01) and followed the guidelines for animal experiments given by the Swedish National Board for Laboratory Animals. Special care was taken to reduce stress and pain on the animals before and during the experimental period. Adult, nine month female New Zealand White (NZW) rabbits weighing between 4,4 – 5,8 kg (I-III) were used.

Surgical procedure and anaesthesia, animal studies (I-III)

In experimental animal studies (I-III), the animals were anaesthetized by intramuscular (i.m.) injections of a combination of phentanyl and fluanizone (Hypnorm®, Janssen, Brussels, Belgium; 0.7 mg/kg body weight (b.wt.) and intraperitoneal (i.p.) injection of diazepam (Stesolid®, Dumex, Copenhagen, Denmark; 1,5mg/kg b.wt.). Lidocaine (5 % Xylocain®, Astra AB Södertälje, Sweden) was infiltrated subcutaneously (s.c.) to obtain local anaesthesia. The limbs were shaved and disinfected with chlorohexidine (5mg/ml, Pharmacia AB, Stockholm, Sweden). Operations were performed under sterile conditions. Each animal received two scaffolds of the same type in one leg and two scaffolds of the other type in the contra lateral

leg. One scaffold was inserted in each proximal tibial metaphysis and one scaffold in each medial femoral condyle according to a random scheme. The bone was exposed separately through skin incisions and blunt dissection of the underlying tissue, including the periosteum. The holes in both the tibia and femur were made using dental implantation drills up to a diameter of 3.8 mm under profuse irrigation with sterile saline (NaCl 9 mg/ml; ACO, Sweden). The scaffolds were then gently pressed in place (Fig 4).

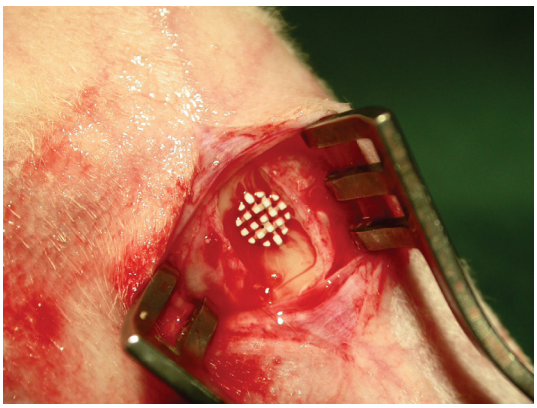

Figure 4
Zirconia scaffold placed in rabbit tibia

The operation site was rinsed with saline and the tissues were sutured in separate layers with Vicryl® 5-0 and finally intracutaneously with Monovicryl® 4-0. Animals were given trimetoprim 40mg + sulfadoxin 200mg/ml (Borgal® vet, Hoechst AB) prior to surgery and two days postoperatively. Analgetics, buprenorphine (Temgesic®, Reckitt and Colman, USA, 0.05mg/ml), were given during three days postoperatively.
Fluorochrome markers for bone formation were given as single injections to the animals in study (II) at two occasions. Oxytetracyclin (Sigma, St Louis, USA) was given at a dose of 25mg/kg b.wt 4 weeks postoperatively; Alizarine complexone (Sigma, St Louis, USA) was given at a dose of 30 mg/kg b.wt. 5 weeks postoperatively.
Animals were killed after 6 weeks with an overdose of barbiturate (Mebumal®, ACO Läkemedel AB, Solna, Sweden) and fixed by perfusion via the left heart ventricle with 2.5% glutaraldehyde in 0.05M sodium cacodylate buffer, pH 7.4. The outline of the experiments is given in Table III.

Table III
Experimental design. Hydroxyapatite (HA), microporous hydroxyapatite (mHA) and zirconia (ZrO_2)

Study number	Number of animals (A)/ humans (H)	Observation time	Defect site	Defect size	Materials
I	8A	6 weeks	Tibia & femur	Ø 3,8 mm	HA, ZrO_2
II	9A	6 weeks	Tibia & femur	Ø 3,8 mm	HA, mHA
III	3A	6 weeks	Femur	Ø 3,8 mm	HA, mHA, ZrO_2
IV	12H	3 months	Maxilla	Ø 3,0 mm	mHA,ZrO_2

Humans
A double masked, randomized, intraindividual, human histological study was approved by the ethical research committee at the Linköping University, Linköping, Sweden (Dnr. M35-05). Twelve patients (six men and six women, 48-72 years old) subjected to dental implant placement in the maxilla were thoroughly informed of the purpose of the study, and thereafter signed an informed consent to participate.

Inclusion/ exclusion criteria
Healthy individuals between 20-75 years old refered for implant treatment in the premolar region of the maxilla were included in the study. Patients with a clinical history of smoking (> 5 per day), immunosuppresive agents, cardiovascular/renovascular drugs, recent cardio vascular disease, hormonal disease, radiotherapy in the head/ neck region and infection were excluded.

Surgical procedure and anaesthesia, human histological study (IV)
Local anesthesia (10-12 ml Xylocain Dental Adrenalin® 2%, 12.5 µg/ml, Dentsply, Skarpnäck, Sweden) was administered in the maxilla. Following crestal incision buccal and lingual muco-periosteal flaps were elevated. Dental implants were placed according to the protocol of the manufacturer. Following a masked randomized insertion scheme, one hydroxyapatite and one zirconia scaffold were placed bilaterally in each patient posterior to the dental implants. 4 mm deep holes were prepared in the maxilla using twist drills up to a diameter of 3 mm under profuse irrigation of sterile saline (NaCl 9mg/ml; ACO, Sweden). The scaffolds (Ø 3mm, height 4 mm) were gently pressed into the prepared holes (Fig 5 A-D). After thorough rinsing with sterile saline the flaps were replaced and sutured with Vicryl® 5-0 (Johnson&Johnson, Sollentuna, Sweden). All patients received analgetics postoperatively (Diclofenac T ratiopharm 50 mg, ratiopharm AB, Helsingborg, Sweden, 3 times daily for 1-2 days). Antibiotics were prescribed for 7 days (either phenoxymethylpenicillin 4 g daily or clindamycin 600 mg daily).

The patients were advised to rinse daily for two weeks with a 0.1% chlorhexidine digluconate solution (Hexident, Ipex, Solna, Sweden).
After three months of healing, the scaffolds were surgically exposed and retrieved with surrounding bone tissue using a trephine drill (inner diameter: 5 mm)

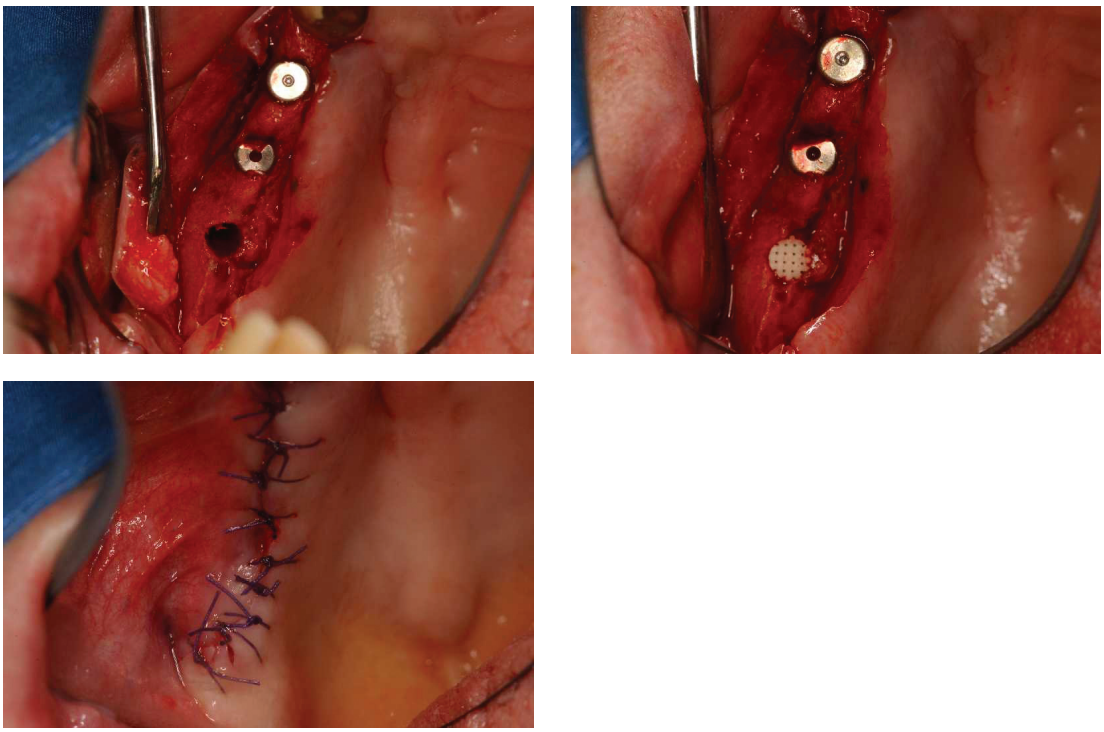

Figure 5 A-C
Photographs demonstrating the defect created in posterior maxilla (A) followed by inserted zirconia scaffold adjacent to titanium implants (B) and final closure of the mucoperiostal flap (C).

Tissue preparation and sectioning techniques

Sample preparation for light microscopy (I-II, IV)

The scaffolds and the surrounding bone were removed and further immersed in glutaraldehyde for 2-4 days. After dehydration in ethanol, the undecalcified specimens were embedded in plastic resin (LR White, The London Resin Co Ltd, Hampshire, UK). The specimens were divided longitudinally by sawing in the centre of the scaffold (Exact cutting and grinding equipment, Exact Apparatebau, Norderstedt, Germany) and ground sections (thickness:15-20µm) prepared and stained with 1% toluidine blue [134,135].

All sections for light microscopy (LM) were analysed by the first author (blinded). The intraexaminer reproducibility for the morphometry was estimated. Measurements were performed at eight different occasions on one section. The standard deviations were used to describe the reproducibility of the examiner.

Sample preparation for scanning electron microscopy (I-IV)

The plastic resin embedded, undecalcified specimens were divided into two blocks longitudinally by sawing, with one of the blocks prepared for scanning electron microscopy (SEM). The tissue blocks were polished with a fine-grained paper (SiC-Paper, grit 4000, Struers A/S Denmark), and coated with a thin conductive carbon layer (thickness about 1000 Å**)** by vacuum evaporation (AGAR SEM Carbon Coater, Germany) prior to the SEM analysis.

Sample preparation for focused ion beam microscopy/transmission electron microscopy (III)

To find suitable areas for transmission electron microscopy (TEM), the scaffold/bone interface was first studied by SEM to define that bone was present and in direct contact with the material (Fig 6 A,B).

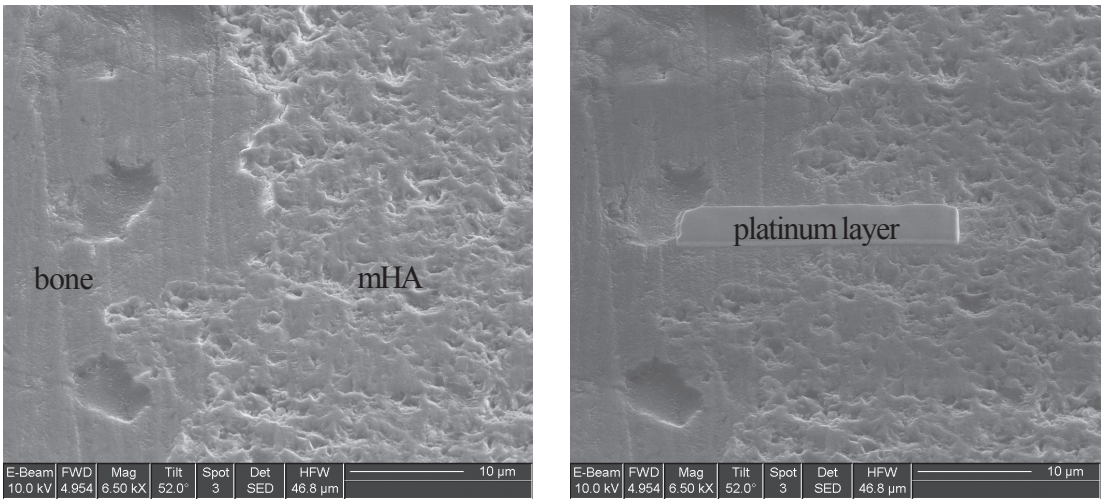

Figure 6 A, B

SEM (FIB) demonstrating a close contact between bone and microporous hydroxyapatite (mHA) (A) and the deposition of platinum on top of region of interest (B).

TEM samples from chosen areas were produced using a dualbeam-FIB, which is a combined FIB and SEM, as follows (Fig. 7 A-D). The procedure is also schematically illustrated in Fig. 8 A-E.

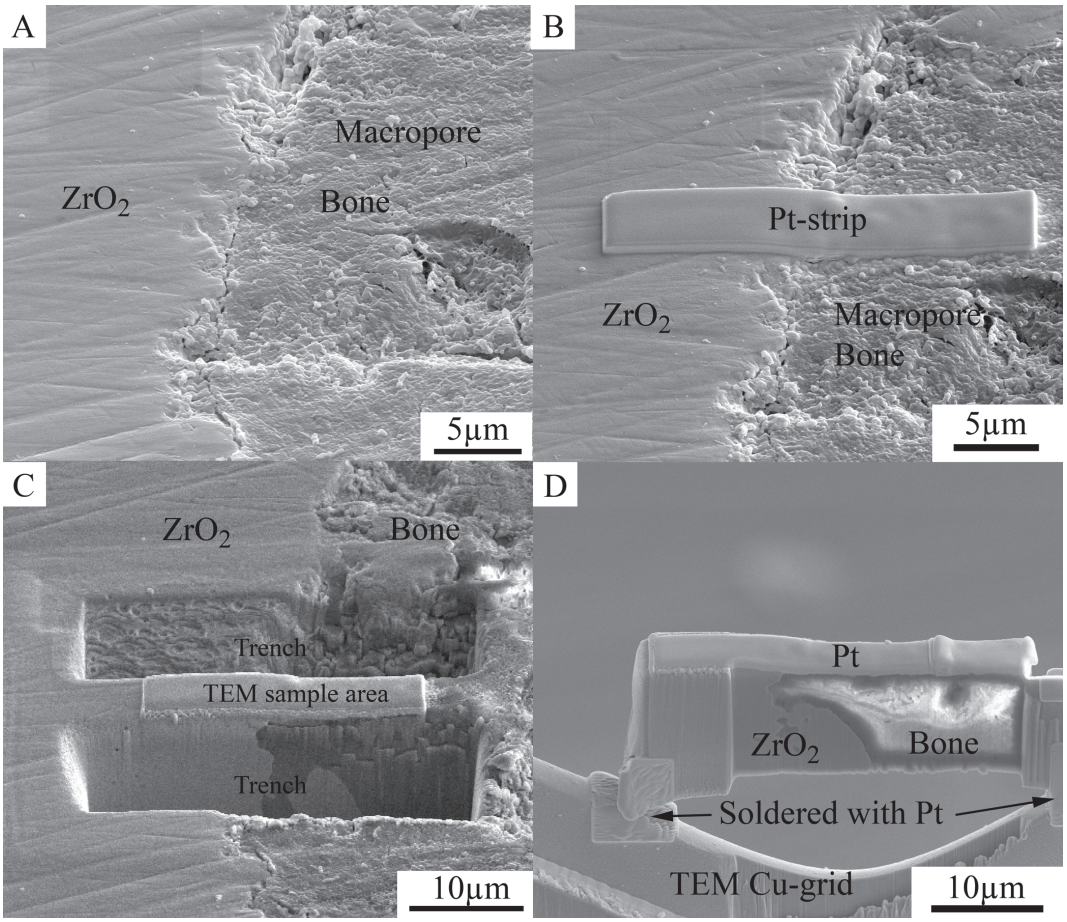

Figure 7 A-D
SEM micrographs of the interface between zirconia and bone (embedded in plastic resin) (A). The region of interest (to be subjected to "sectioning") (B) is slowly deposited by a thin layer (100nm) of platinum (Pt) (length 25µm x width 5µm) by electron beam assisted chemical vapour deposition (CVD). This is done in order to preserve the topmost surface of the subsequent TEM sample from artefacts induced by the ions. It is followed by a rapid Pt deposition of a thick layer (1µm) using the ion beam over the same area. Trenches are dug from both sides of the Pt-coated area (C) using gallium ions, producing a solid piece measuring 25x10x5 µm (length x height x width), containing the area of interest. This piece is subsequently lifted out (in situ) using an Omniprobe micromanipulator and soldered to a v-grooved TEM grid by Pt deposition (D).

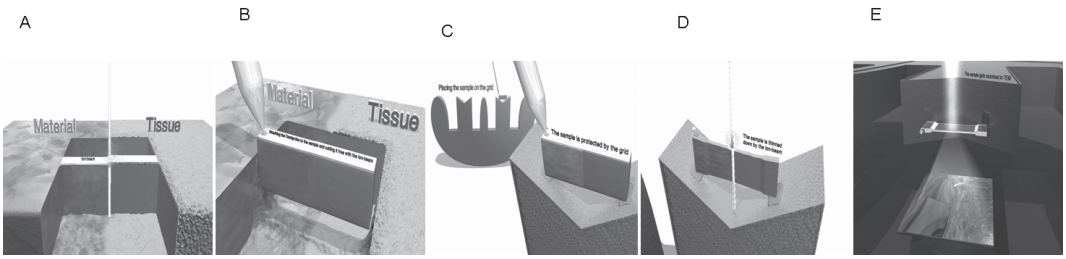

Figure 8 A-E
Schematic pictures illustrating the entire process to TEM evaluation of microporous hydroxyapatite. A suitable implant tissue interface was selected by SEM and milled by FIB (A). A large bar cutout by the FIB was lift-out from the block (B). The bar was soldered to a TEM grid (C). The sample was fine polished to a thickness of about 100nm (D). TEM analysis (E).

For further description of the used method see Ref. [136,137]. The FIB used was a FEI Strata DB235 equipped with electron and an ion column as well as an Omniprobe micromanipulator system. The obtained samples were analyzed in bright field (BF) mode using a JEOL 2000 TEM operated at 200 kV (LaB6 filament). The high resolution and analytical results where obtained in the FEI Tecnai F30 ST operated at 300kV.

LM morphometry
LM morphometry was performed on the ground sections using an Eclipse E600 light microscope (Nikon, Kawasaki, Kanagawa, Japan) and connected computer software.

Animal studies (I-II), human study (IV)
The bone occupying the macropores of the ceramic scaffolds and the amount of bone- to-scaffold contact was calculated. In study (IV) also the bone-to-scaffold contact adjacent the defect border was calculated and compared to the inner bone-to-scaffold parameters of the materials.

Statistics (I-II,IV)
Non-parametrical statistics (Wilcoxon rank sum test) was used in experimental animal studies (I-II) and for the human study (IV). Prior to the human study a power analysis was performed with the assumption to find a 5 units (%) difference between the two materials. The power analyses done showed that to receive an alpha = 0.05 required 12 individuals giving a total power of 88 %. Main parameters were bone area and bone contact (I, II, IV).

RESULTS

Materials

The fabricated scaffolds in study I-III had a diameter of 3,8 mm and a height of 4 mm. Scaffolds used in study IV had a diameter of 3 mm and a height of 4 mm (Table III). In study I-IV the scaffolds had identical macroporosity, consisting of square shaped and interconnected pore channels with a size about 350 microns and a macroporosity around 40 volume %. When cast materials of hydroxyapatite and zirconia were sintered, almost fully dense materials could be obtained (Table IV). The remaining porosity consisted of small closed pores without connections to the surface. It was further possible to influence the sintered density of hydroxyapatite from almost fully dense to highly microporous through control of the colloidal processing conditions. The sintered density of the microporous hydroxyapatite used was around 78 %, where the remaining porosity consisted of open micropores that were interconnected to around 99 % (Table IV). The ceramic scaffolds in study II-IV had protrusions successfully applied bilaterally on top of each scaffolds.

Table IV

Material pore characteristics. Hydroxyapatite (HA), microporous hydroxyapatite (mHA) and zirconia (ZrO_2)

Material	Microporosity (vol %)			Macroporosity (vol %)	Macropore size
	Open	Closed	Total		
HA	0.0	0.8	0.8	40.0	350µm
mHA	22.1	0.2	22.3	40.0	350µm
ZrO_2	0.0	0.7	0.7	40.0	350µm

Chemical composition

X-ray diffraction (XRD) of the hydroxyapatite showed the presence of minor amount of β-tricalcium phosphate while no differences were found between the dense and microporous materials. The zirconia was mainly tetragonal with a small amount of monoclinic phase. This was due to phase transformation that occurs when the dense material was crushed to powder during sample preparation (Fig 9 A, B).

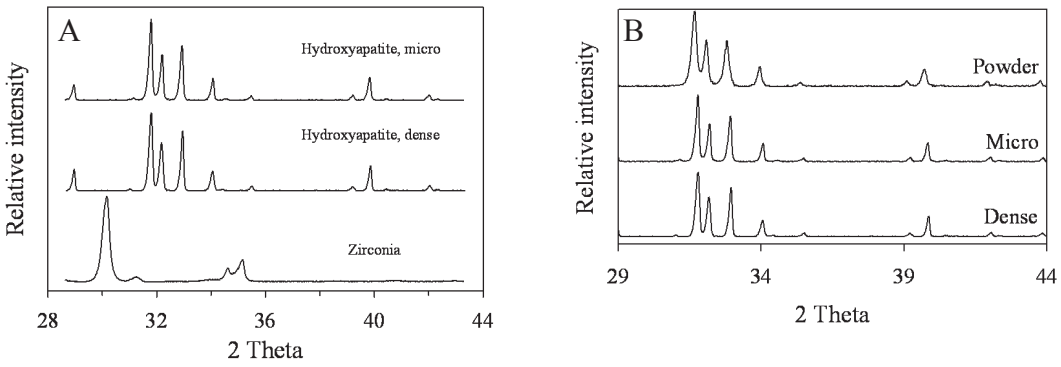

Figure 9 A, B
Diffraction patterns of sintered materials of zirconia and hydroxyapatite (with and without microporosity) (A). Diffraction patterns from the powder and sintered hydroxyapatite (dense and microporous) (B).

Surface topography

The A-side in study I was renamed to the P-side in study II, the same was done for the B-side that was renamed to the O-side, in order to better define the manufacturing directions of the mould (orthogonal or parallel – to manufacturing direction) as the sources of topography (Fig 3 A-C).

The (P) side was rougher than the (O) side inside the macropores irrespective of material, with respect to the S_a value. No differences in roughness could be seen comparing the (P)-side between the three materials. The same was seen for the (O)-side with exception for microporous hydroxyapatite where the (O) - side was somewhat rougher. In hydroxyapatite a surface enlargement for the (P)-side was noted compared to zirconia and microporous (P)-side, as characterised by S_{dr}. A clear orientation of structures could be distinguished for both sides and all materials except for the (O) - side of microporous hydroxyapatite (S_{tr}) (Table. V). The surfaces of the three materials are visualized in (Fig 10 A-F).

Table V

Surface roughness for the three materials representing the orthogonal (O) and paralllel (P) sides inside macropores. Zirconia (ZrO_2), hydroxyapatite (HA) and microporous hydroxyapatite (mHA)

Specimen type	Side	n	Sa (µm)	Sds (µm-2)	Sdr (%)	Str	Sci
ZrO_2	P	30	2.23 (0.78)	0.0094 (0.014)	33.85 (13.57)	0.10 (0.03)	1.53 (0.09)
	O	30	0.51 (0.16)	0.149 (0.011)	9.91 (2.59)	0.17 (0.21)	1.40 (0.15)
HA	P	30	2.54 (0.63)	0.105 (0.008)	200.66 (69.88)	0.46 (0.16)	1.40 (0.20)
	O	30	0.44 (0.10)	0.128 (0.016)	16.72 (5.35)	0.24 (0.18)	1.24 (0.11)
mHA	P	30	2.40 (0.41)	0.103 (0.003)	95.80 (21.92)	0.42 (0.25)	1.52 (0.09)
	O	30	1.70 (0.33)	0.101 (0.005)	79.87 (18.72)	0.66 (0.08)	1.44 (0.09)

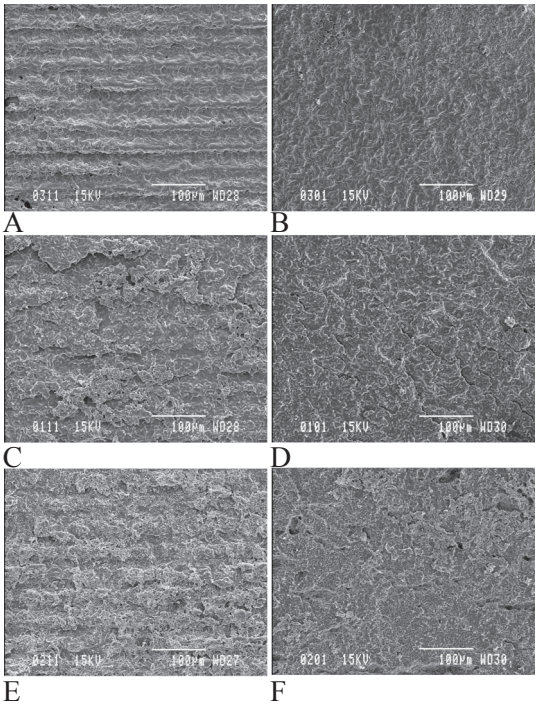

Figure 10 A-F

(A) Topography of P side in zirconia (ZrO_2).

(B) Topography of O side in ZrO_2.

(C) Topography of P side in hydroxyapatite (HA).

(D) Topography of O side in HA.

(E) Topography of P side in microporous hydroxyapatite (mHA).

(F) Topography of O side in mHA.

Sterility and endotoxin content of materials

The minimum β-irradiation dose given was measured to be 25 kGy.
None of the tested materials were contaminated after the cleaning and sterilization procedure. The data is presented in Table VI.

Table VI
Endotoxin content registered with LAL method. Hydroxyapatite (HA), microporous hydroxapatite (mHA) and zirconia (ZrO_2).

Paper	Endotoxin	Materials
I	<0,006 EU/ml	HA, ZrO_2
II	<0,013 EU/ml	HA, mHA
IV	<0,005 EU/ml	mHA, ZrO_2

Macroscopical observations

In animal studies (I-III) all sites healed uneventfully, showing no evidence of inflammatory response to the ceramic scaffold during the experimental period. All scaffolds were well incorporated in bone after 6 weeks. A similar uneventful healing pattern was seen in the human study (IV), though 3 zirconia scaffolds were encapsulated by fibrous tissue at retrieval (without signs of infection). A soft tissue swelling could be noticed in some animals the first day after surgery due to the high permeability of the scaffold, irrespective of material chemistry. This permeability may also explain the bone growth present externally on top of some scaffolds at explantation.
In a few human test objects bone resorption was noted on top of the alveolar ridge exposing the top of the scaffold. This was not seen in femoral and tibial sites in the rabbit model.
With respect to the handling characteristics of the different materials, zirconia scaffolds was experienced to demonstrate more strength than the HA scaffolds. The addition of micropores to hydroxyapatite was also experienced to lower the strength of the material in work bench handling situations. The fit in the created defects was the same for all materials due to the scaling of the moulds prior to sintering which compensated different shrinking patterns of materials used.

Histology

Light microscopy

In the animal studies two different general morphological patterns of bone ingrowth were observed using LM. In the apatite scaffolds the internal macroporosities had bone lining the inner surface of the scaffolds as well as filling the centre portions of the macropores. In contrast, bone was usually observed only as a lining of the inner surface of the internal macroporosities of zirconia. In areas devoid of mineralized bone, bone marrow and/or adipose tissue were detected (Fig 11 A, B).

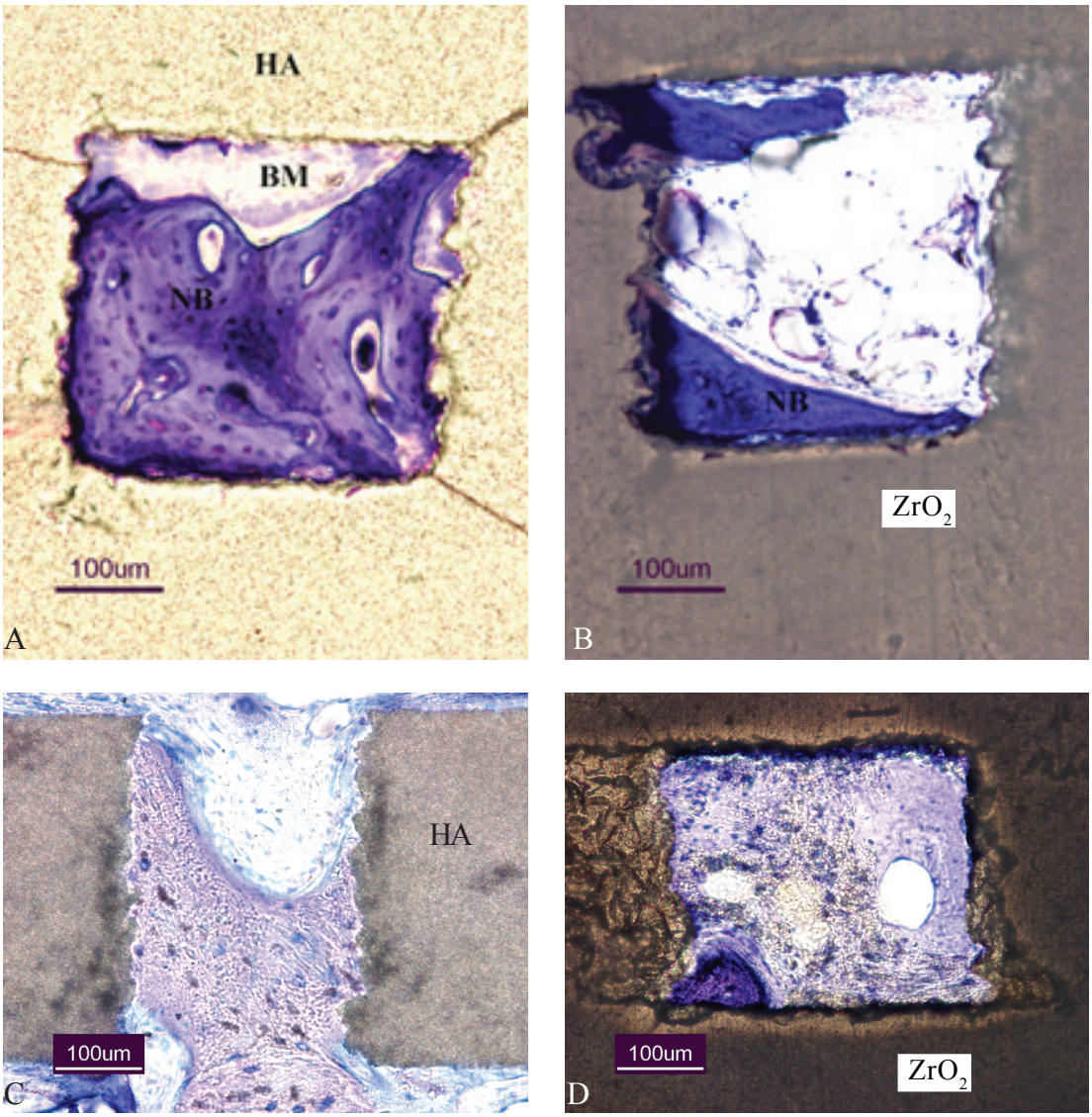

Figure 11
Hydroxyapatite scaffolds (HA) after 6 weeks in rabbit (A) and 3 month in human (C). Zirconia scaffolds (ZrO_2) at same time points in rabbit (B) and human (D).

In the human study (IV) a similar pattern of bone ingrowth as in rabbits (I) could be seen, demonstrating a peripheral pattern of bone ingrowth in zirconia and a more disseminated pattern throughout the apatite scaffold (Fig 11 C, D). The centre of the zirconia scaffolds in human (IV) had more fibrous tissue compared to zirconia scaffolds implanted in rabbits (I) where bone marrow and/or adipose tissue was more often present in areas devoid of mineralized

bone. Regarding the effect of different bone beds used in the animal studies (I-III) the endosteal bone growth was more evident in scaffolds located in the femur than in the tibia. This was notable in particular for hydroxyapatite scaffolds (I).
In tibia, the newly formed bone appeared to have its origin from the endosteal part of the bone and from the defect border (I, II). The two surface roughnesses in each macropore could be distinguished at LM and low SEM level but not at TEM level. The addition of microporosity did not affect the patterns of bone ingrowth or the bone morphology within the apatite scaffolds on the LM level. The micropores in the material were not detectable using LM magnifications (< 40X).

Scanning electron microscopy

A close contact without intervening soft tissue was seen between bone and the chemically different materials in animal studies (I, III). Examination using SEM demonstrated the presence of bone inside macropores of both apatite and zirconia scaffolds. Occasionally, cracks were visible, mainly in the scaffold material of apatites. Cracks were detected at the immediate interface between zirconia scaffolds and bone whereas cracks were seldom detected at the interface between bone and hydroxyapatite scaffold. In the human (IV) study a close contact without intervening structures could be seen for both materials. The location of cracks in these samples was also positioned as in rabbit samples. By using SEM the micropore structure in hydroxyapatite could be visualized demonstrating a pore size of a few microns. In animal (II,III) and human (IV) studies examination using SEM demonstrated bone inside macropores reaching into the outer micropores of hydroxyapatite scaffolds (Fig 12 A,B). Evaluation of the contents of micropores inside the bulk material was not possible using SEM.

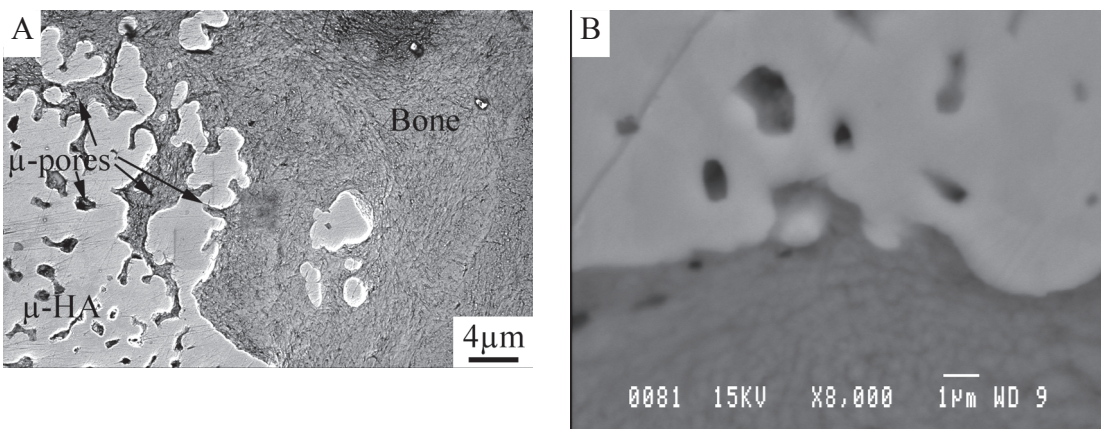

Figure 12 A,B
SEM demonstrating bone ingrowth into the outer micropores of hydroxyapatite in rabbit femur after 6 weeks (A) and human maxilla after 3 months (B).

Transmission electron microscopy

Since no significant qualitative interfacial differences could be detected between the materials when evaluated by SEM, the ultrastructure of the interfaces between bone and the macro- and micro-pores were evaluated using FIB and TEM (III). Overall the bone evaluated by SEM/ TEM did not have an oriented growth of the collagen fibrils and was thereby considered woven. Collagen fibres could be detected inside the macropores of all materials. The border between the ceramic materials and the bone was homogenous without intervening structures under higher magnification. In apatite scaffolds bone was densified close to the material forming a collagen-free layer consisting of fine apatite crystals partly distinct from those in bone. This structure will be referred to as the apatite layer. At high resolution TEM (HRTEM) the well organised crystal structure could be seen in the synthetic hydroxyapatite compared to the randomly organised nanocrystals in the apatite layer (Fig 13).

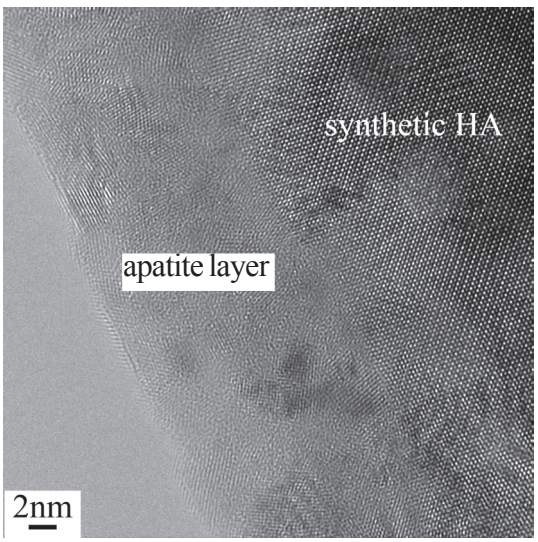

Figure 13

HRTEM of microporous synthetic hydroxyapatite/apatite layer interface in rabbit femur after 6 weeks, demonstrating a well organised crystal structure in the synthetic hydroxyapatite (HA) and fine unorganised crystals in the apatite layer.

In zirconia scaffolds it was not possible to detect an unmineralized zone between bone and material neither could an apatite layer be detected. Using STEM and EDS no differences in Ca/P ratio could be detected between the material, the apatite layer and the bone closest to the interface of the apatite scaffold. Also, as earlier described, the presences of cracks were distributed differently between zirconia and hydroxyapatite materials. In the hydroxyapatite scaffolds the apatite layer was around 200 nm wide. The addition of microporosity to hydroxyapatite scaffold reduced the width of the layer to around 100 nm. At high magnification mineralized tissue could be followed into the outer micropores having a size of around 1 μm.

The inner micropores in hydroxyapatite contained apatite with a fibrillar structure; however characteristic collagen banding was not detected (Fig 14 A,B).

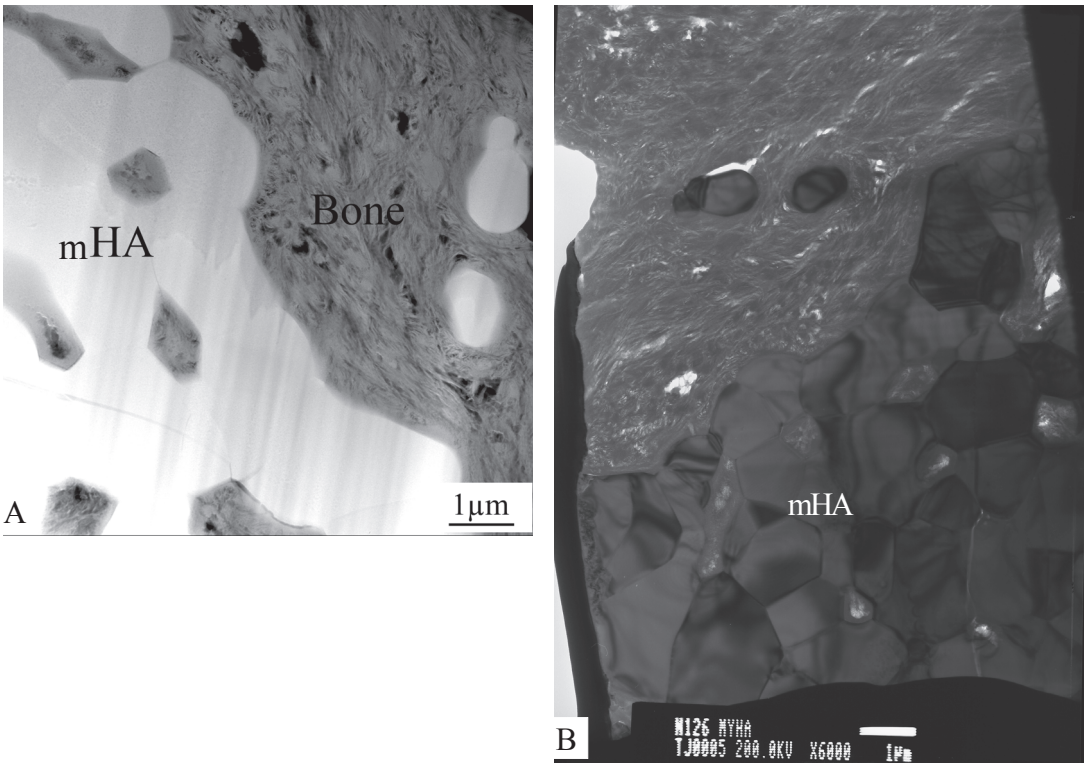

Figure 14 A,B
Scanning electron microscopy mode (STEM) (A) and bright field mode (BFTEM) (B) of microporous hydroxyapatite (mHA) in rabbit femur after 6 weeks - demonstrating bone ingrowth in outer micropores.

Using STEM and EDS no differences in Ca/P ratio could be detected between the tissue inside the micropores compared to the surrounding synthetic hydroxyapatite material. Carbon was detected inside the micropores of the bulk material as well as in the bone of the macropores using electron energy loss spectroscopy (EELS). No carbon was detected in the apatite material itself using the same technique. It remains to be determined if the carbon is tissue or resin specific.

Histomorphometry (LM)
In the rabbit model the bone response, as judged by histomomorphometry, inside apatite scaffolds was 2-3 times larger compared to zirconia scaffolds (I). This difference was even greater in the human maxilla (IV) where a 4-7 times larger bone response was seen in apatite scaffolds compared to zirconia scaffolds (Fig 15 A, B).

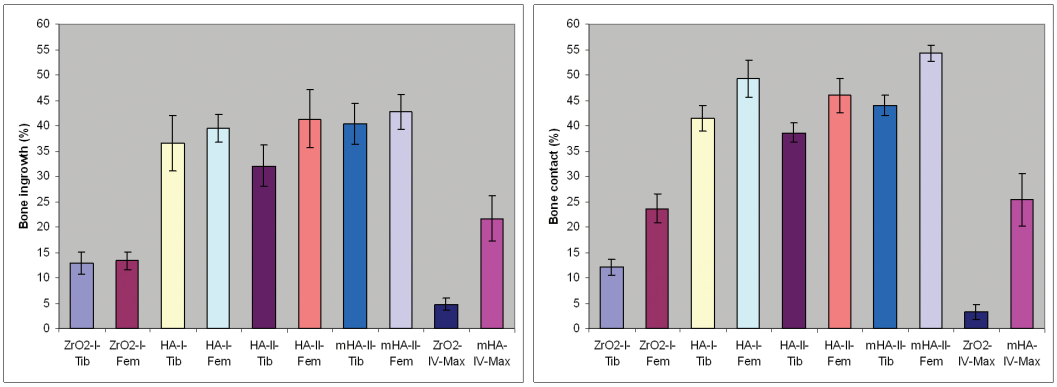

Figure 15 A, B
Results from study I, II (6 weeks) and IV (3 months) regarding bone ingrowth (A) and bone contact (B) for zirconia (ZrO_2), hydroxyapatite (HA) and microporous hydroxyapatite (mHA) in tibia (Tib), femur (Fem) and maxilla (Max).

The presence of microporosity significantly increased the bone contact inside the apatite scaffolds in rabbits at 6 weeks (II). No significant difference in the bone area parameter was detected between the two apatite materials, with or without open microporosity, irrespective of implantation site in rabbits (II) (Fig 15 A). When individually evaluating the effect of the different surface roughness values in the macropores of each material, no difference in bone-to-scaffold contact could be evaluated.
As described in M&M, to determine the precision of reading, eight repeated measurements on one section were carried out. The results of these measurements revealed a mean area of 17,8 % +/- 0,8% standard deviation and a mean contact of 48,1 % +/- 1,5 % standard deviation.

DISCUSSION

Role of material chemistry on the bone response in porous ceramics

The results of the present thesis have shown that material chemistry is decisive for the outcome of bone regeneration inside ceramic scaffolds manufactured by Free Form Fabrication. The investigated hydroxyapatite scaffolds in both rabbits (6 weeks) (I) and humans (3 months) (IV), demonstrated significantly greater amount of bone contact and bone ingrowth compared to zirconia scaffolds.

To evaluate the effect of different scaffold materials requires that the scaffolds used have the same geometrical characteristics in order to exclude confounding factors. In the present thesis this was possible by using the Free Form Fabrication technique to produce identical macroporous scaffolds with the same external shape, inner macroporous shape, size and interconnectivity.

In the present study, zirconia was selected on the basis of being an inert material. Zirconia has also recently been suggested as a suitable high strength material in contact with bone [37]. There is an obvious interest in gaining more information about the bone response towards this material, particularly on the ultrastructural level, before patients are treated with zirconia implants in contact with bone.

In humans (IV) 3 zirconia scaffolds did not integrate in bone due to fibrous encapsulation. Whether this was due to an inferior bone quality of the patient or the properties of the material is not clear. Since no similar pattern of encapsulation of the hydroxyapatite scaffolds was found in the same patients, it is suggested, but not proven, that the zirconia scaffolds had a less bone promoting effect, underscoring the role of material chemistry. At present, it cannot be excluded however, that non-optimal, local healing conditions at implantation sites in the human maxilla could have played a role.

Although a direct bone contact was detected for all materials using SEM, the analysis by TEM showed distinctly different structural properties at the interfaces. The observations underscore the necessity to aim for a thorough characterization on different levels of resolution. The ability of a material to achieve a bond with bone leads to beneficial properties since the properties of the material then can guide the appropriate clinical use. In hydroxyapatite samples bone was in contact with hydroxyapatite through a collagen-free layer consisting of fine apatite crystals partly distinct from those in bone. The crystals of this apatite layer and those of bone were intermingled at their surface, suggesting chemical bonding. The present thesis extends previous observations on the interface between bone and zirconia [37,38], demonstrating for the first time a different ultrastructure since an apatite layer – detected on the surface of hydroxyapatite - was not found on zirconia. The results in paper III suggests that the absence of the apatite layer in zirconia could be due to the inert, non-toxic chemical nature of zirconia. Also, comparing the interfaces of zirconia and hydroxyapatite, a tendency of crack propagation was more often detected in the case of zirconia. This might indicate a weaker bonding at the

interface or the mere presence of only physical bonding in the case of zirconia. In hydroxyapatite scaffolds the interface was stronger than the material itself, as judged by the morphological evaluation.

Role of macro- and microporosity on the bone response in ceramics

A pore within a ceramic material can vary depending on size, shape, interconnectivity, surface chemistry and roughness. The mechanisms whereby ceramic pore parameters stimulate new bone formation are not known. The present thesis showed that chemistry and microporosity provide an environment suitable for promoting the bone regeneration inside a ceramic porous structure. The choice made in this thesis regarding the identical macropore size (350 μm) of the scaffold was based on the literature [64,69,71], This macropore diameter was used as a "locked" parameter throughout all studies, allowing studies on the effect of chemistry and open microporosity. Bone ingrowth was detected in macropores of all materials with a significant increase in bone response for scaffolds made of apatite material. Apart from the chemistry and pore size it has been suggested that also other structural parameters like the morphology and connectivity of pores might promote the bone response [43,45,46,57,58]. This was noted in some specimens where a notable amount of new bone formation was present on top of the cortex. One can not exclude that the high permeability, as a result of the interconnectivity of the scaffolds, elevated the repositioned flap, creating a void stimulating additional bone formation. Since this kind of bone formation was seen in all materials it is unlikely to be a result of the material chemistry but rather due to the identical interconnected macrogeometry. However, whether it is a permanent bone formation outside the skeletal envelope due to the permeability of the scaffold design has not been possible to prove due to only one test period and macropore size used in each study. Regarding the small amount of remaining microporosity in non-microporous hydroxyapatite, they consisted of closed pores and would thus not influence the biological response.

It was also possible to influence the sintered density of hydroxyapatite from almost fully dense to highly microporous through control of the colloidal processing conditions. This demonstrated the possibility to add microsized interconnections without receiving differences in chemical composition of the materials. The microporosity variations in different ceramic/tissue studies have usually been created by altering the sintering process [73,76] or the shaping process[70]. This will apart from altered content of microporosity also result in alteration of other material characteristics such as the grain size. As a result, there is an uncertainty in the literature regarding the effect of microporosity on the bone response [69,70]. The present results have shown that the addition of open micropores in otherwise identical hydroxyapatite scaffolds promote the bone contact.

Though, since bone ingrowth also was prominent within the non-microporous hydroxyapatite scaffolds, microporosity is not as decisive regarding the total bone response in the same way as chemistry. The use of more chemically inert materials might further isolate the effect of

microporosity. This has partly been done by Sennerby [38] where coatings with different levels of microporosity did not promote the bone response to zirconia dental screw implants in rabbits.

Furthermore, ultrastructural findings in the present thesis demonstrated that the bone /material interface had a thinner apatite layer in hydroxyapatite scaffolds with an open microporosity (III). There is at present, no clear explanation for this observation. A possible explanation is that the micropores favour a cell milieu not demanding such a wide formation of apatite layer for optimal circulation adjacent to the cells (osteoblasts) as in dense hydroxyapatite. SEM/ TEM analysis also revealed bone inside micro-size microporosities of the microporous hydroxyapatite. This is in agreement with recent data presented by Porter et al. [83] where mineralized collagen fibres had grown into the strut porosity of porous hydroxyapatite implants after 6 weeks in vivo.

In inner micropores (separated from the macroporous surface in sections) the distinction between bone and apatite layer was not clear-cut. A combination of larger FIB samples and immunocytochemistry could be one alternative for further studies on the precise composition of these micropores. Since mineralized fibrils had grown into the strut porosity of the microporous hydroxyapatite, a consequence for the biomechanical strength on the micron level could be anticipated. This would give a possibility of better biomechanical anchorage of microporous hydroxyapatite in bone.

Controlling pore roughness of the surfaces inside scaffolds is difficult. Due to the manufacturing process the surface roughness of hydroxyapatite and zirconia was almost similar. Different surface roughness was obtained for the orthogonal and parallel surfaces within the macropores of each material. Interestingly, no difference in bone contact was detected between the orthogonal and parallel surfaces within the macropores of each material. A possible error in evaluating surface roughness on these kinds of ceramics can be examplified with the results presented for the microporous hydroxyapatite (II). Optical interferometry showed lower surface enlargement (Sdr) for microporous hydroxyapatite compared to the dense hydroxyapatite. One explanation is that each analytical method has certain drawbacks and evaluating micropores on a ceramic surface using this technique could be one of them. Another possible error could be the small area evaluated at each measurement. However, a large number of areas were measured on each specific material and the goal of the measurements was to gain objective data of the ceramic surface structure on the micrometer level. There is at present no explanation to the finding that different surfaces inside the macropore of each material did not significantly affect the bone contact. Similar results have been presented evaluating zirconia dental screws with different surface roughness [38]. However, there is to the authors´ knowledge no available data regarding the effect of different surface roughness inside scaffolds of any material. This is partly due to the difficulty in manufacturing and tailoring the properties of pores as well as reflecting the difficulty in measuring the surface roughness of the walls of pores. It would be desirable to evaluate a homogenous pore topography within each macropore, thereby more easily discriminating the effect of topography. Generally, the different investigations found in

the literature are difficult to compare in order to define an optimal pore size, shape, interconnectivity, surface chemistry and roughness. The Free Form Fabrication technique used in this thesis could be a suitable tool for the evaluation of optimal pore properties for tissue ingrowth.

Aspects on models and methods

Animals

In the present thesis, adult, New Zealand White (NZW) female rabbits were used in all animal studies I-III. The animal model allowed scaffold installation in created cortical and trabecular bone defects. When bone regeneration is studied, rabbits are general advantageous too small rodents since e.g. mice and rats have a more primitive bone structure, which does not include Haversian system. Other factors that affect the bone formation are e.g. gender, age, anatomical location and how the animals are kept [138]. The animals in studies I-III were all sacrificed at 6 weeks observation time. The strategy in the present thesis was to minimize the number of observation times and to study relatively early effects of different materials. At this time period, new bone formation occurs and the healing process is in an active phase. In addition, several previous studies concerning bone remodeling and implant-bone interactions have used this animal model, insertion local and time period, demonstrating that the model allows a determination of the bone response and discrimination between different material surface properties [139,140].

Humans

The patients enrolled in the human study (IV) matched the inclusion criteria, thereby avoiding health disorders as well as local intra-oral circumstances that might interfere with the healing process. The experimental protocol followed the surgical procedures planned for the conventional two-stage oral implant rehabilitation. Compared to rabbits the human have about 2-3 times slower bone formation, remodelling and maturation [141]. A clear advantage was the possibility to obtain the scaffold with bone using a trephine drill in conjunction with the abutment connection surgery. Additional "pure" bone biopsies and X-rays would presumably have given valuable information with regard to the activity and anticipated host response on an individual level. The effects of scaffold positioning (inserted crestally) on the results are not known. However, a resorption of the crestal part of the alveolar bone was clinically noted in some samples compared to the situation present in the rabbit bone. Furthermore, both the animal and human scaffolds were functionally unloaded. It is however difficult to control the loads and forces in animals or humans where the process of osteogeneses was the main interest.

Design of scaffolds

The cylinder, press-fit design of the scaffold has the risk of movements as a potential drawback. This may result in soft tissue encapsulation. A screw-shaped design usually provides a good initial implant stability. In the present thesis the evaluation of bone regeneration was made inside the 3 dimensional scaffolds. The designed scaffolds, handled correctly histotechnically, also permitted a larger individual area/contact (surrounded by material) to be evaluated by histomorphometry, than possible to achieve and evaluate using a screw design with the same external dimensions.

Histology

Qualitative and quantitative histology in the present thesis has been performed on one section per specimen with main purpose to search for statistically significant differences between pairs of test and control scaffolds. Undecalcified ground sections prepared according to the technique of Donath and Breuner [134,135] were used. The thin sections (10-15 μm) [142] and staining allowed reproducible and reliable results with discrimination between old and newly formed mineralized tissue. The use of fluorochromes (II), labelling the mineralization phase of hard tissues [143], demonstrated that the bone was woven and that bone had started to form and remodel at 4 weeks inside the scaffolds (II). The precision of reading revealed no statistically significant intraexaminer differences.

SEM/ FIB/TEM

SEM enabled a valuable overview of bone-scaffold relationships. In addition, micron-sized micropores facing the macropores in both rabbit (II) and human (IV) were infiltrated by bony tissue and all materials in both species demonstrated a direct bone-to-material contact, as judged by SEM. This ultrastructure was further unravelled by observations of an apatite layer on hydroxyapatite in contrast to zirconia, using FIB/TEM.

TEM samples from the interface between bone and hydroxyapatite/zirconia, respectively, were successfully produced using the FIB preparation technique. The technique has previously been applied to titanium implants with ultra-thin hydroxyapatite coating inserted in bone [86], calcium aluminate ceramics inserted in both bone [144] and teeth [145], titanium amputation prostheses [146] and native, commercially available, oral implants [147]. A significant advantage with the FIB technique is the possibility to perform ultra-thin sectioning of interfaces between hard materials, such as metals, and undecalcified bone. In the present study, the possibility to produce intact ultra-thin sections for TEM analysis of interfaces between brittle ceramics and bone was clearly appreciated. The intact sectioning of the micropores was a prime example. An important conclusion from the present analytical work was the necessity to perform survey analytical observations in lower magnification using SEM prior to defining the regions of interest for FIB. The small size of the FIB samples underscores this necessity.

Aspects on Free Form Fabrication

As mentioned in the literature review there are several methods available for the production of designed ceramics. Designed implant/scaffolds will improve the possibility to perform controlled studies of evaluating bone-material responses in vivo. The technique of Free Form Fabrication is rapidly growing and it is hard to determine what directions the future will take. The Free Form Fabrication technique chosen in this thesis has a high precision and has worked well producing almost fully dense materials with defined macroporous geometry. Other techniques may be faster and more suitable for industrial manufacturing. The purpose in the present studies has been to design and manufacture controlled research tools to evaluate material - bone reactions. Taken together, the possibility to freely select both material and geometry is likely to revolutionize the future research on functional biomaterials in clinical applications.

Future

A selection of important topics for future research within the field of Free Form Fabrication and tissue regeneration are:

1. to optimize chemistry and porosity (micro- and macro sized) to suit specific biological environments;
2. to use Free Form Fabrication methods to make biomedical objects, built to fit a particular anatomical defect, grown to shapes by medical images (CT/MRI), perhaps with sophisticated interior configuration;
3. to balance the tissue response with the mechanical properties of the material through a variation of geometry and composition;
4. to stimulate the tissue reactions in vivo and in vitro (tissue engineering) through modulation of the microenvironment and resorbability of the delivery vehicle (scaffold);
5. to evaluate the mechanisms of early (within days and weeks) bone formation within micro- and macropores using additional techniques, for example RT-PCR and immunohistochemistry, complementary to LM, SEM, and FIB/TEM.

SUMMARY AND CONCLUSIONS

1. Free Form Fabrication of ceramic scaffolds enabled systematic studies on the role of material chemistry and microporosity for bone regeneration.
2. Focused ion beam microscopy enabled the preparation of ultra-thin sections of undecalcified bone – ceramic scaffold specimens, allowing ultrastructural characterization of intact specimens of bone and porous ceramic materials.
3. Scaffold material chemistry had a significant effect on promotion of bone ingrowth and bone contact.
4. An open microporosity had a significant effect on bone contact.
5. Depending on scaffold material chemistry and open microporosity the ceramic - bone interfaces displayed different ultrastructure.
6. The biological effects (bone ingrowth and bone contact) of scaffold chemistry and microporosity were similarly expressed in the human maxilla and in experimental animals.

In conclusion,
the present study demonstrate that material chemistry and macro- and microporosity of Free Formed Fabricated ceramic scaffolds are decisive parameters for bone contact and ingrowth.

ACKNOWLEDGEMENTS

I would like to thank all who have been involved in the work with this thesis, in particular:

Peter Thomsen, for his great knowledge, curiosity and guidance throughout my PhD work.

Erik Adolfsson, for great guidance in the field of ceramics and life in general. Also, a special thanks to the rest of the Adolfsson family (Åsa, Astrid and Agnes) for always making me feel welcome.

Elisabeth Liljensten, for introducing me to the wonders of research, great friendship and scientific discussions.

Christer Slotte, for never failing encouragement, innovative mind and clinical guidance.

Lena Emanuelsson and Anna Johansson for great friendship, fun moments and skilled help during surgery and in the laboratory.

Tobias Jarmar and Håkan Engqvist, for your guidance in the word of microscopy and great contributions.

Anna Arvidsson, for valuable contributions and excellent surface analyses.

Ola Norderyd, for valuable contributions.

Keraminstitutet IVF in Mölndal for, all support, SEM analyses-Lars Eklund, and excellent courses.

Magnus Hakeberg and Christoffer Cromvik, for valuable statistical advice.

Lars Sennerby, Thomas Albrektsson, Ann Wennerberg and Carina Johansson-for always trying to answer my questions and creating a nice atmosphere.

Maria Hoffman, for layout.

Barbro Lanner for assistance with administrative matters.

My collegues Luiz, Anders, Felicia, Sofia, Sandra, Shams, Cecilia, Sara, Marco, Omar, Christina, Victoria, Anna G, Jonas, Andreas, Amir, Young- Taeg, Byung-Soo, Patricia, Petra, Ann and Gunilla for joy and support during this work.

My friends at, Malmström/ Norrman Dental Clinic in Varberg, Folktandvården Kulan in Gothenburg and specialisttandvården in Jönköping and Halmstad, for outstanding support and clinical guidance.

I would also like to thank my family, Gustav, my son - for being you-I love you. Inger, Göran, Ulf and Eva for good advise in life. Jacob my brother for good discussions, Karin, Per, Christine, Christoffer and Julia – for being there when I needed them.

Charlotte, my love, to whom this thesis is dedicated, for your patience, encouragement and giving me the strength to keep on.

My Ph.D. graduate student work was supported by the Hjalmar Svensson Reasearch Foundation, The Swedish Research Council (K2006-73X-09495-16-3), The Institute for Postgraduate Dental Education, Jönköping and the Institute for Biomaterials and Cell Therapy (GöteborgBio and Vinnova VinnVäxt Program).

REFERENCES

[1] JA.Buckwalter, Bone Joint surg 77-A (1995) 1256.
[2] L. Schweiberer, H. Stutzle, H.K. Mandelkow, Arch Orthop Trauma Surg 109 (1989) 1.
[3] L.Ollier, Paris, Victor Msson et Files, 1867, Volumes I and II (1867).
[4] R. Burwell, History of bone grafting and bone substitutes with special reference to osteogenic induction, Butterworth-Heinemann Ltd, Cambridge, 1994.
[5] A. Barth, Archive fur klinische Chirurgie 46 (1893) 409.
[6] H. Burchardt, Clin Orthop Relat Res (1983) 28.
[7] E.H. Groeneveld, J.P. van den Bergh, et al, J Biomed Mater Res 48 (1999) 393.
[8] J.T. Killian, L. Wilkinson, S. White, M. Brassard, J Pediatr Orthop 18 (1998) 621.
[9] A.L. Ladd, N.B. Pliam, J Am Acad Orthop Surg 7 (1999) 279.
[10] J.L. Russell, J.E. Block, Orthopedics 22 (1999) 524.
[11] C.R. Richardson, J.T. Mellonig, M.A. Brunsvold, et al, J Clin Periodontol 26 (1999) 421.
[12] K. Majtenyi, Orv Hetil 137 (1996) 2895.
[13] V.M. Goldberg, S. Stevenson, Clin Orthop Relat Res (1987) 7.
[14] T. Albrektsson, C. Johansson, Eur Spine J 10 Suppl 2 (2001) S96.
[15] JB. McCarthy, J. Lida, LT. Furcht, Mechanisms of parenchymal cell migration into wounds, Plenum Press, New York, 1996.
[16] R. Adell, U. Lekholm, K. Grondahl, et al, Int J Oral Maxillofac Implants 5 (1990) 233.
[17] L.P. Nystrom E, Forssell A, Kahnberg KE, Int J Oral Maxillofac Surg 24 (1995) 20.
[18] E.D. Arrington, W.J. Smith, H.G. Chambers, et al, Clin Orthop Relat Res (1996) 300.
[19] E.M. Younger, M.W. Chapman, J Orthop Trauma 3 (1989) 192.
[20] C.N. Cornell, Orthop Clin North Am 30 (1999) 591.
[21] J. Brandt, R. Carlsson, Il. Ekberg, S. Karlsson, et al, Keramguiden, Svenska Keraminstitutet, Göteborg, 1989.
[22] L.F. Peltier, Clin Orthop 21 (1961) 1.
[23] C.J. Damien, J.R. Parsons, J Appl Biomater 2 (1991) 187.
[24] R. Leriche, A. Policard, The normal and pathological physiological physiology of bone and its problems., Henry Kimpton, London, 1928.
[25] P. Ducheyne, J Biomed Mater Res 21 (1987) 219.
[26] K. De Groot, Ann N Y Acad Sci 523 (1988) 227.
[27] C.P. Klein, A.A. Driessen, K. de Groot, et al, J Biomed Mater Res 17 (1983) 769.
[28] C.A. van Blitterswijk, J.J. Grote, W. Kuypers, et al, Biomaterials 6 (1985) 243.
[29] A.S. Posner, Clin Orthop Relat Res (1985) 87.
[30] A.S. Posner, J Biomed Mater Res 19 (1985) 241.
[31] M. Jarcho, Clin Orthop (1981) 259.

[32] P. Valentini, D. Abensur, B. Wenz, et al, Int J Periodontics Restorative Dent 20 (2000) 245.
[33] R.Z. LeGeros, Clin Orthop Relat Res (2002) 81.
[34] W. Bonfield, Doyle C, Tanner K.E, In vivo evaluation of hydroxyapatite reinforced polyethylene composites., Elsevier science, Amsterdam, Netherlands, 1986.
[35] W. Schulte, B. d´Hoedt, Z Zahnärtztl Implantol 3 (1988) 167.
[36] W. Schulte, Quintessence Int 15 (1984) 1.
[37] J. Mellinghoff, ZZI - Zeitscrift fur Zahnärztliche Implantologie 4 (2006) 288.
[38] L. Sennerby, A. Dasmah, B. Larsson, et al, Clin Implant Dent Relat Res 7 Suppl 1 (2005) S13.
[39] C. Piconi, G. Maccauro, Biomaterials 20 (1999) 1.
[40] L.C. Leon Y, Adv Colloid Interface Sci 76-77 (1998) 341.
[41] Y. Kuboki, H. Takita, D. Kobayashi, et al, J Biomed Mater Res 39 (1998) 190.
[42] B.J. Story, W.R. Wagner, D.M. Gaisser, et al, Int J Oral Maxillofac Implants 13 (1998) 749.
[43] J.J Klawitter, J Biomed Mater Res 5 (1971) 161.
[44] A. Uchida, S.M. Nade, E.R. McCartney, et al, J Bone Joint Surg Br 66 (1984) 269.
[45] P.S. Eggli, W. Muller, R.K. Schenk, Clin Orthop (1988) 127.
[46] J.X. Lu, B. Flautre, K. Anselme, et al, J Mater Sci Mater Med 10 (1999) 111.
[47] B.S. Chang, C.K. Lee, K.S. Hong, et al, Biomaterials 21 (2000) 1291.
[48] T.M. Chu, D.G. Orton, S.J. Hollister, et al, Biomaterials 23 (2002) 1283.
[49] J.J. Klawitter, J.G. Bagwell, A.M. Weinstein, et al, J Biomed Mater Res 10 (1976) 311.
[50] R.S. Ling, A.J. Timperley, L. Linder, J Bone Joint Surg Br 75 (1993) 693.
[51] R. Holmes, V. Mooney, R. Bucholz, et al, Clin Orthop Relat Res (1984) 252.
[52] K.A. Hing, S.M. Best, W. Bonfield, J Mater Sci Mater Med 10 (1999) 135.
[53] R.E. Holmes, Plast Reconstr Surg 63 (1979) 626.
[54] R.B. Martin, M.W. Chapman, N.A. Sharkey, et al, Biomaterials 14 (1993) 341.
[55] O. Gauthier, J.M. Bouler, E. Aguado, et al, Biomaterials 19 (1998) 133.
[56] G. Daculsi, N. Passuti, Biomaterials 11 (1990) 86.
[57] J-H Kuhne, R. Bartl, B Frisch, et al, Acta Orthop Scand 65 (1994) 246.
[58] K.A. Hing, S.M. Best, K.E. Tanner, et al, J Mater Sci Mater Med 10 (1999) 663.
[59] W. Hubbart, Thesis, Marquette University, Milwaukee, 1974.
[60] M. Bohner, G.H. van Lenthe, S. Grunenfelder, et al, Biomaterials 26 (2005) 6099.
[61] T.D. Roy, J.L. Simon, J.L. Ricci, et al, J Biomed Mater Res A 66 (2003) 283.
[62] K.U. Lewandrowski, J.D. Gresser, S. Bondre, et al, J Biomater Sci Polym Ed 11 (2000) 879.
[63] Y. Kuboki, Q. Jin, H. Takita, J Bone Joint Surg Am 83-A Suppl 1 (2001) S105.
[64] E. Tsuruga, H. Takita, H. Itoh, et al, J Biochem (Tokyo) 121 (1997) 317.
[65] H.E. Gotz, M. Muller, A. Emmel, et al, Biomaterials 25 (2004) 4057.

[66] S.F. Hulbert, F.A. Young, R.S. Mathews, et al, J Biomed Mater Res 4 (1970) 433.
[67] S. Kujala, J. Ryhanen, A. Danilov, et al, Biomaterials 24 (2003) 4691.
[68] J.P. Fisher, J.W. Vehof, D. Dean, et al, J Biomed Mater Res 59 (2002) 547.
[69] K.A. Hing, B. Annaz, S. Saeed, et al, J Mater Sci Mater Med 16 (2005) 467.
[70] A.L. Rosa, M.M. Beloti, P.T. Oliveira, et al, J Mater Sci Mater Med 13 (2002) 1071.
[71] K.A. Hing, S.Saeed, B.Annaz, et al, Key Engineering Materials (2004) 254.
[72] B. Annaz, K.A. Hing, M. Kayser, et al, J Microsc 215 (2004) 100.
[73] A. Bignon, J. Chouteau, J. Chevalier, et al, J Mater Sci Mater Med 14 (2003) 1089.
[74] A. Boyde, A. Corsi, R. Quarto, et al, Bone 24 (1999) 579.
[75] K.A. Hing, S.M. Best, K.E. Tanner, et al, J Biomed Mater Res A 68 (2004) 187.
[76] P. Habibovic, H. Yuan, C.M. van der Valk, et al, Biomaterials 26 (2005) 3565.
[77] M. Rouahi, O. Gallet, E. Champion, et al, J Biomed Mater Res A 78 (2006) 222.
[78] K.A. Hing, S.M. Best, K.E. Tanner, et al, J Mater Sci Mater Med 8 (1997) 731.
[79] M. Tre´cant, J. Dele´crin, G.Daculsi, Clin Mater 15 (1994) 233.
[80] W.A. Dellinger JG, RD. Jamison, J Biomed Mater Res A Jun 1 (2006) 563.
[81] H.A. Woodard JR, SK. Lan, Biomaterials Jan 28 (2007) 45.
[82] W.J. Landis, M.C. Paine, M.J. Glimcher, J Ultrastruct Res 59 (1977) 1.
[83] A.E. Porter, T. Buckland, K. Hing, et al, J Biomed Mater Res A (2006).
[84] S.F. Giannuzzi LA, Introduction to Focused Ion Beams: Theory, Instrumentation, Applications and Practice., Kluwer Academic, Boston, 2004.
[85] M.W. Phaneuf, Micron 30 (1999) 277.
[86] H. Engqvist, G.A. Botton, M. Couillard, et al, J Biomed Mater Res A (2006).
[87] L.L. Hench, J. Am. Ceram. Soc., 81 (1998) 1705.
[88] Hench, J. Am. Ceram. Soc., 74 (1994) 1487.
[89] S. Hench , Allen, J. Biomed Mater Res 2 (1978) 117.
[90] J.F. Osborn, H. Newesely, Biomaterials 1 (1980) 108.
[91] M. Neo, S. Kotani, Y. Fujita, et al, J Biomed Mater Res 26 (1992) 255.
[92] D.G. Legeros RZ, In vivo tranformation of biphasic CaP ceramics:Histological, ultrastrucltural and physico-chemical characterization, CRC Press, Boca Raton, 1990.
[93] K. T, Thermochim Acta 280 (1996) 479.
[94] L.L. Hench, Bioceramics, Butterworth-Heinemann, Oxford, 1994, p. 3.
[95] X. Liu, A. Huang, C. Ding, et al, Biomaterials 27 (2006) 3904.
[96] J. Malmström, T. Jarmar, E. Adolfsson, et al, In manuscript..
[97] S. Kotani, Y. Fujita, T. Kitsugi, et al, J Biomed Mater Res 25 (1991) 1303.
[98] M. Neo, T. Nakamura, C. Ohtsuki, et al, J Biomed Mater Res 27 (1993) 999.
[99] K. Hayashi, K. Uenoyama, N. Matsuguchi, et al, J Arthroplasty 4 (1989) 257.
[100] K. Ono, T. Yamamuro, T. Nakamura, et al, Biomaterials 11 (1990) 265.
[101] Y.S. Chang, M. Oka, T. Nakamura, et al, J Biomed Mater Res 30 (1996) 117.
[102] T. Suzuki, M. Hukkanen, R. Ohashi, et al, J Biosci Bioeng 89 (2000) 18.

[103] Y. Akagawa, R. Hosokawa, Y. Sato, et al, J Prosthet Dent 80 (1998) 551.
[104] Y. Akagawa, Y. Ichikawa, H. Nikai, et al, J Prosthet Dent 69 (1993) 599.
[105] R.J. Kohal, D. Weng, M. Bachle, et al, J Periodontol 75 (2004) 1262.
[106] A. Scarano, F. Di Carlo, M. Quaranta, et al, J Oral Implantol 29 (2003) 8.
[107] L. Sennerby, L.E. Ericson, P. Thomsen, et al, Clin Oral Implants Res 2 (1991) 103.
[108] L. Sennerby, P. Thomse, LE. Ericsson, J Mater Sci Mater Med 3 (1992) 262.
[109] T. Albrektsson, CB. Johansson, L. Sennerby, Periodontology 4 (2000) 58.
[110] J.D. de Bruijn, C.P. Klein, K. de Groot, et al, J Biomed Mater Res 26 (1992) 1365.
[111] F.B. Bagambisa, U. Joos, W. Schilli, J Biomed Mater Res 27 (1993) 1047.
[112] P. Ducheyne, J.M. Cuckler, Clin Orthop Relat Res (1992) 102.
[113] J.D. de Bruijn, CA. van Blitterswijk , J Biomed Mater Res 29 (1995) 89.
[114] JE. Daavies, Int J Proshodont 11 (1998) 391.
[115] M. Neo, S. Kotani, T. Nakamura, et al, J Biomed Mater Res 26 (1992) 1419.
[116] R.Z. LeGeros, Legeros, J.P., in L.L. Hench, Wilson, J. (Editor), An Introduction to Bioceramics, World Scientific, Singapore, 1993, p. 139.
[117] L.L. Hench, Anderson,in L.L. Hench, Wilson, J. (Editor), An introduction to Bioceramics., World Scientific, Singapore, 1993, p. 41.
[118] Y. Leng, J. Chen, S. Qu, Biomaterials 24 (2003) 2125.
[119] LL. Hench, An introduction to bioceramics, World Scientific, London. UK, 1993.
[120] LL. Hench, Life Chem Rep 13 (1996) 187.
[121] M.Ogiso, J.Dent. Res 60 (1981) 419.
[122] M.Ogiso, H. Kaneda, J. Arasaki, et al, in Trans.Soc.Biomat 4, 54, 1981.
[123] J.F. Osborn, H. Newesly, Dynamic aspects of the implant-bone interface, in Dental implants, Carl Hansen Verlag, Muchen, 1980.
[124] LL. Hench, in Founders Award, Society for Biomaterials 24th annual meeting, San Diego, CA, 1998, p. 511.
[125] LL. Hench, in W.J. Hench LL, eds. (Editor), World Scientific, Singapore, 1993.
[126] H.A. Ratner BD, Schoen FJ et al., in H.A. Ratner BD, Schoen FJ, Lemons JE, eds. (Editor), Biomaterials Science, Academic Press., New York, 1996.
[127] T.M. Chu, J.W. Halloran, S.J. Hollister, et al, J Mater Sci Mater Med 12 (2001) 471.
[128] J.J. Beaman, J.W.Barlow, D.L. Bourell, Solid freeform fabrication: a new direction in manufacturing, Kluwer, Dordrecht, 1997.
[129] P.F. Jacobs, Rapid prototyping and manufacturing - fundamentals of stereolithography, 1st edn; Society of Manufacturing Enginineers., Dearborn , MI, 1992.
[130] W. Palm, Prototyping primer, TLF, Penn State, 2002.
[131] Printed with kind permission by my friend Erik Adolfsson.
[132] T.J. Schek RM, Hollister SJ, Krebsbach PH, Orthod Craniofacial Res 8 (2005) 313.
[133] J.W. Halloran, British Ceramic Transactions 98 (1998) 299.

[134] K. Donath, G. Breuner, J Oral Pathol 11 (1982) 318.
[135] K. Donath, Der Präparator 34 (1988) 318.
[136] RJ. Patterson, D. Mayer, L. Weaver, et al, Microsc Microanal 8 (2002) 566.
[137] T. Jarmar, A. Palmquist, R. Brånemark, et al, J Dent Res Submitted (2006).
[138] JA.Love, Lab Animal Sci 44 (1994) 5.
[139] C. Larsson, Thesis, Institute of Anatomy and Cell Biology, Göteborg University, Gothenburg, 1997.
[140] S.M. Mohammadi, Thesis, Department of Biomaterials, Institute for surgical Sciences, Göteborg University, Gothenburg, 2003.
[141] E. Roberts, L. Gareetto, N Brezniak, Bone physiology and metabolism., Mosby Year Book, St.Louis, 1994.
[142] CB.Johansson, Thesis, Biomaterials Group, Department of Handicap Research, University of Göteborg, Göteborg, 1991.
[143] E.A. Tonna, Bone tracers: Cell and tissue level techniques., Academic Press, New York, 1979.
[144] H. Engqvist, M. Couillard, GA. Botton, Trends Biomater. Artif. Organs 19 (2005) 27.
[145] H. Engqvist, J.E. Schultz-Walz, J. Loof, et al, Biomaterials 25 (2004) 2781.
[146] T. Jarmar, A. Palmquist, R. Brånemark , et al, Submitted Clin Ortho and Rel Res (2007).
[147] A. Palmquist, T. Jarmar, L. Emanuelsson, Clin Implant Dent Relat Res Accepted for publication. (2007).